cerege
CENTRE EUROPÉEN
DE RECHERCHE ET D'ENSEIGNEMENT
DES GÉOSCIENCES DE L'ENVIRONNEMENT

AIX-MARSEILLE-UNIVERSITÉ UM34 – CNRS UMR 7330 – IRD UMR 161
- COLLÈGE DE FRANCE (CHAIRE ECO) – INRA USC 1410
TECHNOPOLE ENVIRONNEMENT ARBOIS MEDITERRANEE
AVENUE LOUIS PHILIBERT
13545 AIX-EN-PROVENCE CEDEX 4
TEL : 04 42 97 15 00 – FAX : 04 42 97 15 05

Marie Laugié, corresponding author.
marielaugie@gmail.com

Pau, Friday 17th of April 2020

Dear Martin Claussen,

Please find enclosed the revised manuscript and supplementary material for your consideration as a contribution in *Climate of the Past:*

*"Stripping back the Modern to reveal the Cenomanian-Turonian climate and temperature gradient underneath"*

The manuscript and supplementary material have been corrected regarding the comments of the two reviewers and according to suggestions made in our response to comments. You will find below the point-by-point response to reviewers' comments as well as a marked-up manuscript version.

In addition to minor changes described in our response to reviewers, here are the main changes made in the manuscript:

(1) Precision on the studied period, that is the Cenomanian-Turonian (and not the whole Cretaceous). We replaced Cretaceous by Cenomanian-Turonian in the title and in the text.
(2) Modifications of the experimental design section in order to gain clarity, by creating two separate sections for (a) boundary conditions and (b) initial conditions. We reorganized the description to be clearer and added some precisions.
(3) The choice of choosing a linear factorization was justified and discussed in the introduction of the Results Section.
(4) We reorganized the section 4.1 (model/data comparison) by separating atmospheric and oceanic results into two distinct paragraphs to gain clarity.
(5) We made a separate section for the discussion on temperature gradients (Section 4.2). We added precisions on the Cretaceous / Eocene gradient comparison and we removed the last paragraph of this part to avoid repetitions with the Results.
(6) Conclusions were shortened to avoid repetitions with the results/discussion.
(7) Supplementary figures were added to give more details on results and studied processes.
(8) About the copy-editing comment, our native English co-author went through a hard proofing to ameliorate the formulation ang gain clarity.

Yours sincerely,
Marie Laugié, on behalf of all co-authors.

**Detailed point-by-point response :**

## Anonymous Referee #1

### 1 General comments

First, it is a bit unclear to me whether the presented results are supposed to be representative for the Cretaceous in general (as suggested by the title of the manuscript), or for the Cenomanian-Turonian, or for the Oceanic Anoxic Event 2.

→ The results presented here are representative only for the Cenomanian-Turonian. Simulations for Early Cretaceous or Late Cretaceous (Maastrichtian) would imply different boundary conditions (e.g. paleogeography). It may be not clear enough in the manuscript, we will clarify it by changing "Cretaceous" to "Cenomanian-Turonian" in the title and in the manuscript.

In the discussion section, due to a lack of other Cenomanian-Turonian simulations, the results are also compared to results for the Eocene, which occurred much later in time than the Cretaceous; but the boundary condition differences between these different time slice simulations are not discussed appropriately.

→ Indeed, the boundary conditions are different for the Eocene and the comparison of gradients cannot be done directly. The idea was more to have a discussion on the temperature gradients simulated by Earth System Models in general.

While the applied approach of successively changing the boundary conditions is appreciated and useful here, and a lot of extra work, the authors do not appropriately discuss any potential shortcomings of the applied linear factorization approach. For example, in a warmer climate like that with $4xCO_2$, a reduction of the surface albedo due to the removal of continental ice sheets would probably have a larger effect, because the surface albedo effect would be masked to a lesser extent by snow cover. I.e., the contributions can depend on the sequence of the changes.

→ You are correct. We agree that repeating the experiments with a different sequence of changes would be desirable to fully assess the shortcomings of the linear factorization method. It indeed has been suggested that a different sequence of boundary condition changes would probably give different results (Lunt et al., 2012). However, these additional experiments using the IPSL-CM5A2 earth system model require a computational cost that we cannot afford.

We have added the following discussion about linear factorization in the revised manuscript:

*"The choice of applying a linear factorization approach was made for problems of computing time and cost. Changing the sequence of changes or applying a symmetrical factorization as in Lunt et al (2012) would require too many supplementary simulations. However, such a method is very dependent on the sequence of changes, and results would be probably different if boundary conditions were change in a different order* (Lunt et al., 2012)*".*

As the conclusions (Section 5) are written now, they are a summary (repetition) of the previously presented results (except for the last two sentences, which to me sound like general speculative remarks). I think the conclusions could be worked out more clearly and in more detail, in particular with the questions in mind that are

raised in the introduction. For example, do the results contribute to a consensus on the relative importance of $CO_2$ versus paleogeography (introduction, paragraph starting on page 3 line 78)?

→ We will rearrange the conclusion in order to be less repetitive with the previous sections, but also to be more coherent with the questions raised in the introduction.

**2 Minor / specific comments**

Abstract, page 1 line 14: Please replace "suffered" by something more objective, such as "experienced".

→ Done.

Abstract, line 17: As far as I understand the Cretaceous is a period and not an era.

→ We replaced « era » by « period » where needed throughout the revised manuscript.

Page 2, line 55: What is the "conundrum of Cretaceous $pCO_2$ question"?

→ We meant that atmospheric pCO2 levels are not well constrained in the Cretaceous with a large spread in the values inferred from proxy data (e.g. Wang et al. ESR 2014, Foster et al. Nat Comm. 2017). The sentence was rephrased as follows:
*"Modelling studies have also focused on estimating Cretaceous atmospheric CO2 levels (Barron et al., 1995; Poulsen et al., 2001, 2007; Berner, 2006; Bice et al., 2006; Monteiro et al., 2012) in an attempt to refine the large spread in values inferred from proxy data (<900 to >5000 ppm)."*

Page 4, line 10: Are the carbon and biogeochemical cycle models / is PISCES also running in the presented simulations? Will the results be described elsewhere? In this context, any missing feedbacks could be discussed. E.g., in reality, a 4-fold $pCO_2$ increase would certainly also affect the ice sheets.

→ PISCES is also running but results will be presented in another paper in the near future. Based on previous published results by members of our group (Ladant and Donnadieu, 2016), we have considered that no ice-sheet could be formed at 4-fold pCO2 during the C-T.

Page 5-6, experimental design: The prescribed boundary condition changes could be described in more detail. How exactly is the ice removed? What happens to the water? Is the ocean salinity adjusted in any of the simulations? What are the properties of the bare soil (e.g., albedo)? What happens to the river routing? To understand the simulated surface warming, an estimate of the pure surface height / lapse rate effect would also be helpful. What are the initial conditions for the $4xCO_2$ runs, why are they only "similar" to those described by Lunt et al.? It is not clear to me how ORCHIDEE works in the presented simulations; are the PFT distributions prescribed and do they stay the same thereafter in all simulations?

→ We will rearrange the description of boundary conditions to improve clarity and readability. In simulations with a preindustrial geography, polar ice sheets were removed by setting the fixed land ice fraction to 0 in the model. The topography has been changed accounting for isostatic rebound resulting from the loss of the land ice beneath the Greenland and Antarctic ice sheets. In place of the ice, soil and vegetation parameters were

prescribed to brown bare soil (no vegetation), for which the albedo is derived from the soil color (Krinner et al., 2005). River routing stays unchanged.
We will add supplementary figures of the new topography without ice sheets and of the temperature change due to the lapse rate effect.
Oceanic initial conditions in simulations with 4x CO2 concentrations are adapted from Lunt et al., 2017. In fact, the constant initial salinity field (to 34.7 PSU) is identical to that proposed by Lunt et al. 2017 but the initial ocean temperature field is slightly different from that of Lunt et al. 2017 because of stability issues in the model. We therefore use the following temperature conditions (see also Sepulchre et al., GMD 2020, in review) :

If depth ≤ 1000 m:

$$T = 10 + \left(\frac{1000 - depth}{1000}\right) * 25\cos(latitude)$$

if depth > 1000 m :

T = 10

In our simulations, vegetation in ORCHIDEE is semi-dynamic in the sense that PFTs are prescribed and cannot change but plant phenology is predicted by the model based on surface climate conditions.

Page 6, line 61: TSI in SOLAR-experiment 1351 or 1353W/m2 as in Table 1?

→ Corrected to 1353 W/m2.

Page 8, line 189-190: ...progressive change... induces a general global warming...: this is not true, solar forcing causes cooling.

→ Indeed, the change in solar forcing induces a cooling as indicated on line 195. The general global warming mentioned here refers to the global temperature change in the last simulation (4X-Cretaceous) relative to the first simulation (preindustrial), that is, the summed effect of all boundary condition changes.

Page 8, line 191 and Table 2: It does not make any sense to me to describe the warming in terms of the percentage of the initial temperature. The total warming should be set to 100% here. The following contributions should be described accordingly, too. That means, for example, $CO_2$ contributes 9°C or about 80% to this total warming (and not 61%).

We agree that this section was confusing and we will change it in the revised manuscript.
To include the impact of solar forcing (cooling), which is opposite to those of other boundary condition changes, we had chosen to describe the temperature changes in terms of percentage of the cumulative absolute temperature change. However, as it is confusing, we decided to remove the percentages and to keep only the raw temperature values.

Page 8-9, Table 2: The global anomaly rows are somewhat confusing with the different units ( C versus %). Respective rows showing the relative contributions of the changes (ice, $CO_2$, ...) to the temperature, albedo, emissivity would be useful. That would also help to double-check if the contributions add up to 100%.

→ We removed the percentages that were expressed in terms of initial value percentage and keep only the raw values to avoid confusions.

| | piControl | 1X-NOICE | 4X-NOICE | 4X-NOICE-PFT-SOIL | 4X-NOICE-PFT-SOIL-SOLAR | 4X-CRETACEOUS |
|---|---|---|---|---|---|---|
| T2M (°C) | 13.25 | 13.75 | 22.75 | 23.55 | 21.75 | 24.35 |
| Planetary Albedo (%) | 33.07 | 32.61 | 28.79 | 28.27 | 28.66 | 27.13 |
| Surface Albedo (%) | 20.13 | 19.02 | 16.56 | 15.46 | 15.35 | 14.94 |
| Emissivity (%) | 62.01 | 61.7 | 57.51 | 57.14 | 57.77 | 57.04 |

*Table 2: Simulations results (Global annual mean over last 100 years of simulation.*

Page 9, lines 214-215: A decrease of the snow cover over continents probably does not explain the warming over the polar oceans.

→ Modified sentence: "*First, a decrease of sea ice and snow cover (especially over Northern hemisphere continents and along the coasts of Antarctica) leading to surface albedo decrease, explains the warming amplification over polar oceans and continents."*

Page 9, line 218-220: "The relative humidity decrease can be driven by the temperature rise...". Maybe this is just my lack of meteorological knowledge; references?

→ This part of the manuscript is indeed not very clear. We would need to go into details regarding the changes in water content, relative/specific/absolute humidity as well as atmospheric dynamics to explain the observed changes. We do not want to go into such details in the manuscript which is already long and which not specifically focus on the impact of a CO2 increase, so we finally decided to remove this paragraph.

Page 9, lines 220-226: Are the prescribed processes speculative, or have they been identified in the presented simulation?

→ The processes are identified in the simulation, however, as explained for the previous comment, we finally removed this paragraph from the manuscript.

Page 10, line 241: "These contrasted climatic responses to the impact of ice sheets on sea surface temperature have been observed in previous modelling studies but their origin is still unclear..." A discussion of the different suggested mechanisms compared to the processes at work here would be interesting. Is that possible?

→ We do not detail here the processes responsible for the contrasted climatic response to the ice sheet absence (or presence) as the simulated impacts are mostly regional, and because the climatic consequences of the absence/presence of ice sheets at the poles are already the focus of other studies (Goldner et al., 2014; Knorr and Lohmann, 2014; Kennedy et al., 2015; Kennedy-asser et al., 2020). In these studies, as well as in our simulations, local changes in winds are observed, probably due to topographic changes linked to the existence of the ice sheet. These changes in wind may locally impact oceanic currents, deep-water formation and oceanic heat transport, and thus explain the regional contrasts in temperature changes around the Antarctic continent.

We added some precisions in the manuscript to briefly describe these processes:

*"These contrasted climatic responses to the impact of ice sheets on sea surface temperatures have been documented in previous modeling studies (Goldner et al., 2014; Knorr and Lohmann, 2014; Kennedy et al., 2015). Their origin in the Southern Ocean is still unclear but, in these studies as well as in our simulations, it seems that local changes in winds, due to topography change after polar ice cap removal, are impacting locally oceanic currents, deep-water formation and thus oceanic heat transport and temperature distribution. In the Northern Hemisphere, the observed cooling over Eurasia could be linked to stationary wave feedbacks due to the change in topography after Greenland ice cap removal (See supplementary information; see also Maffre et al., 2018)."*

Page 10, lines 259-260: "These trends are linked to a general decrease of planetary albedo and/or emissivity, ..." Maybe maps of the prescribed surface albedo, actual surface albedo (with snow and ice), and planetary albedo for some of the different simulations would be helpful to follow the argumentation in this section.

→ Supplementary figures of planetary and surface albedo as well as emissivity will be provided.

Page 10, line 261: Which trend is compensated exactly?

→ The increase in albedo, which drives cooling during summer, is compensated by a strong emissivity decrease during winter, leading to winter warming.
Modified sentence in the manuscript: *"This increase in albedo is compensated by a strong atmosphere emissivity decrease during winter but not during summer, which leads to the seasonal pattern of cooling and warming (See Supplementary Figure S5)."*

Page 11, line 267: The Drake Passage still looks open to me in Fig. 2. Maybe it is better to plot the geographies on the model grid, also showing the sea-land mask?

→ Indeed, the Drake Passage is not completely closed but is very shallow (<300 meters of water depth). This configuration essentially shuts down the ACC, as observed on figure 7.

Page 12, line 299: "...increase is due to...", it seems more appropriate to write that it is "consistent with" those previous findings by Rose and Ferreira; or is this evident from the presented simulations?

→ Modified sentence: "*This high-altitude cloudiness increase is consistent with the extratropical increase in OHT…"*

Page 12, lines 310-314: The warming due to the different boundary condition changes does not add up to 100% (49% + 30% - 16% + 4% = 67%). Please check the numbers.

→ The 30% is wrong and should be 31%. However, we finally decided to remove the percentages as it was confusing.

Page 12, lines 314-317: "... the increased contribution of paleogeography in the simulated sea surface warming compared to the atmospheric warming, which is probably driven by the major changes simulated in the surface circulation (Fig. 7)." I think this is an interesting hypothesis that could be elaborated in more detail, because the results to test this hypothesis are available here. Regarding the present-day North Atlantic, I suspect that the large

cooling patch in that area in the CT-simulation (Fig. 4f) could be due to the lack of a Gulf Stream or North Atlantic current equivalent. I.e., in that case, the changed circulation leads to a high-latitude cooling rather than to a warming.

→ The cooling patch observed in the Northern part is located over the Greenland and is due to ocean becoming land in the CT simulation. The cooling patch observed in the Arctic (North of Greenland) could be indeed due to changes in circulation in the North Atlantic. However, this is a regional effect that does not dominate the global signal. The Cretaceous simulation is globally warmer at these latitudes regarding the latitudinal temperature gradients for both winter and summer seasons (fig 6). We do not want to go into details for such regional effects, as they are too numerous to explain, and we want to stay focus on the global signals.

Page 12, line 320: How exactly are the meridional temperature gradients calculated? (T(30 )-T(80 ))/50 , without any averaging applied? Why between 30 and 80 , and not between equator and poles?

→ The meridional gradients are indeed calculated by doing (T(30)-T(80))/50. No average is applied, the values 30° and 80° where chosen to be coherent with the Upchurch et al., 2015 study.

Page 12, line 325: ...the SST gradient can be visualized (not explained) by...

→ Modified sentence: "*The progressive flattening of the SST gradient can be visualized by superimposing the zonal mean temperatures of the different simulation and by adjusting them at the Equator (Fig 9b).*"

Page 13, line 355: To me it looks like the local warming due to the removal of the Greenland ice sheet would have a visible effect on the meridional temperature gradient, but this effect is somewhat counterbalanced by the cooling in Europe and Siberia. As mentioned earlier, I think it would be interesting to elaborate on the processes at work here (e.g., stationary wave feedback?).

→ Indeed, the observed cooling can be due to modifications of stationary waves, at least for the continental part of Eurasia (see figure below). This cooling is however very weak (<1.5°C) compared to the warming observed over Greenland (up to 20°C). We added the precision to the manuscript and will add the following figures to supplementary information:

*"In the Northern Hemisphere, the observed cooling over Eurasia could be linked to stationary wave feedbacks due to the change in topography after Greenland ice cap removal (See supplementary information; see also Maffre et al., 2018)."*

*Geopotential height (m) at 850 hPa for piControl and 1X-NOICE simulations and corresponding anomaly.*

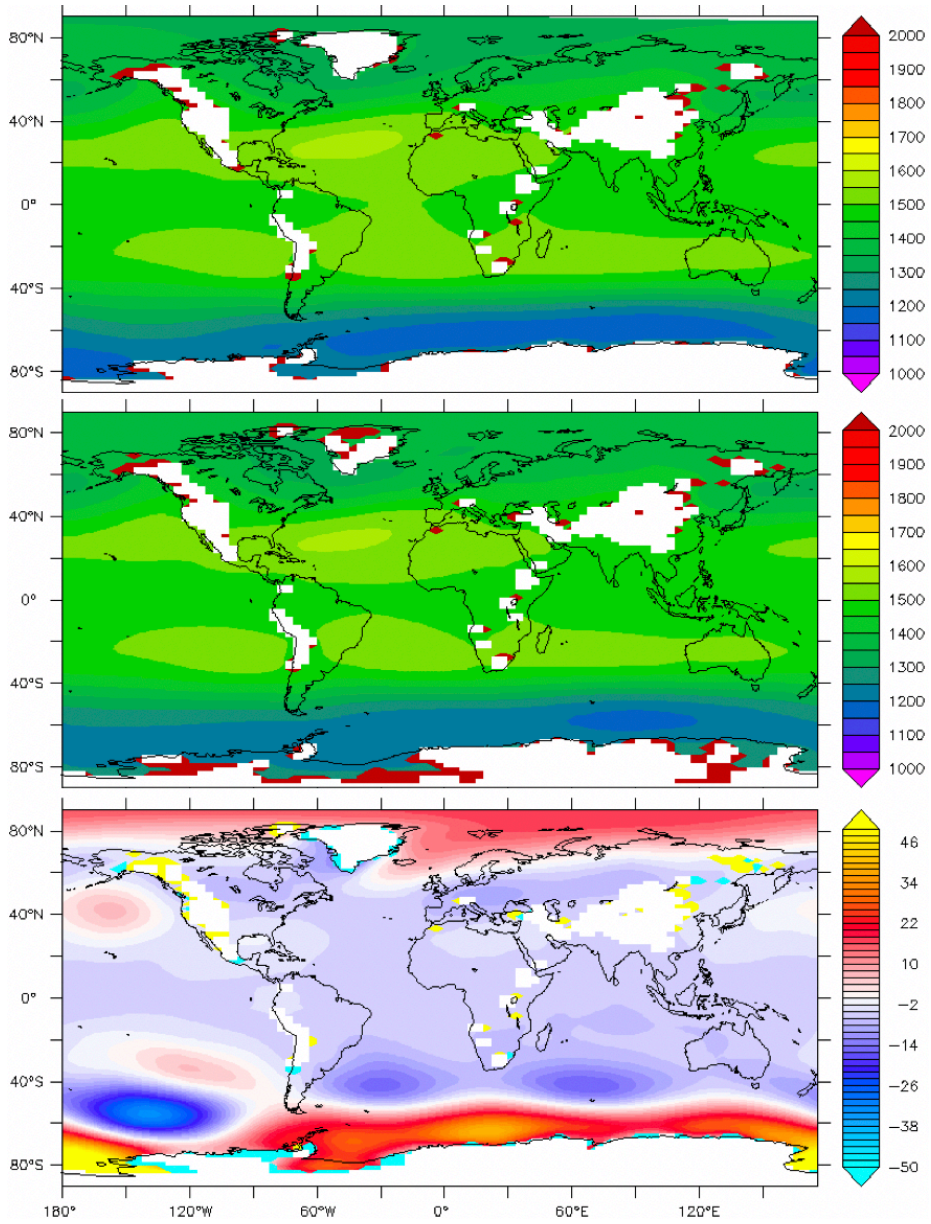


Page 13, lines 360-362: I do not agree. Looking at Fig. 4f, the warming at 40-70 S appears to be more pronounced in the proto-Indian Ocean than over proto-Australia, i.e., the enhanced warming is probably not due to the larger continental area.

→ Indeed, the warming is more pronounced over ocean than over proto-Australia. This warming can be explained by the increased southward oceanic heat transport (cf Results - p.11 – line 277). We modified the paragraph to include this result:

*"In the mid- to high-latitudes of the Southern Hemisphere, the increase in poleward OHT and in the continental area fraction in the CT drive a reduction in the steepness of the atmospheric gradient."*

Page 13, lines 362-363: Again, I don't agree that this should be only an effect of the ocean area (but also, for example, due to the lack of a Gulf Stream or North Atlantic current equivalent).

→ Here, we analyze the global signal, and do not look individually at the different basins. Considering that the global ocean heat transport stays stronger for the Cretaceous (even without Gulf Stream - figure 8c), we don't rely changes in circulation to a lack of paleogeography impact on atmospheric gradient flattening.

Page 14, Section 4.1 A large part of this so-called discussion section is a comparison of the presented model results to previously published proxy data – the section should probably be titled accordingly.

→ New title :
4.1 ABOUT THE CENOMANIAN-TURONIAN CLIMATE : MODEL/DATA COMPARISON

Page 14, line 369: This is not really a prediction, but rather a hindcast; "were compared" meaning "are here compared"?

→ Modified sentence: *"The results predicted by our CT simulation are here compared to reconstructions of atmospheric and oceanic paleotemperatures inferred from proxy data (Fig 10a,b)."*

Page 14, line 370-371: What exactly does "essentially based on Tabor et al. 2016" mean? What are the differences?

→ Most of the data used here for the comparison come from Tabor 2016, and we added some other points from more recent studies. All the references are indicated in the supplementary data.
→ Modified sentence: *"Our SST data compilation is modified from Tabor et al (2016), with additional data from more recent studies (see Supplementary data)."*

Page 14, line 383: Comparison shown in Fig. 10, not 9a?

→ Yes

Page 14, lines 393-394: It could make the discussion of the data-model fit and of the wide spread of temperatures in one latitudinal band easier if the proxy data was also shown on a 2D map (like Fig. 4f). The DSDP locations could then also be marked.

→ We are working here in terms of latitudinal gradients, that's why we didn't want to make the 2D map that would give another direction to the manuscript.

Page 14, line 400: Between 25 and about 28 (not 30) C according to Fig. 10a?

→ Yes

Page 15, lines 407-409: This is a main point and conclusion of the study, and should be worked out in more detail. "...we observe the same underestimate...", same as whose / same as what? The temperatures are compared to proxy data, not observations.

→ Modified sentences: *"The simulated annual SSTs reach a monthly maximum of 28°C around the location of site DSDP 258. We speculate that a seasonal bias in the foraminiferal record may represent a possible cause for this difference, as may local deviations of the regional seawater $d^{18}0$ from the globally assumed -1‰ value. The same trend is observed for atmospheric temperatures with data indicating higher temperatures than the model at high latitudes in both the Southern and Northern Hemispheres. This inter-hemispheric symmetry in model-data discrepancy could indicate a systematic cool bias of the simulated temperatures."*

Page 15, lines 410-416: How exactly are the gradients computed from proxy data? Please add a measure of uncertainty, the range of the reconstructed temperatures for most latitudinal bands is very large.

→ The gradients are calculated based on the slope of the linear regression line (see supplementary data 1). We added in the supplementary file the standard error for the regression line.

Page 15, lines 424-425: "... with the lowest latitudinal gradients being obtained for the highest $pCO_2$ values." This is not correct according to Fig. 11. The lowest gradient seems to be computed for the 6x$CO_2$ CCSM3 simulation. Also, for example, the 2x$CO_2$ Eocene simulation with ECHAM5/MPIOM shows a lower northern hemisphere temperature gradient than any of the 2, 3, 4, 5, or 6x Cretaceous simulations with ECHAM5/MPIOM. Note that the simulation denoted here as ECHAM5 is actually also an ECHAM5/MPIOM run. This illustrates that the differences in the applied boundary conditions between the simulations other than $CO_2$ play a large role and should be discussed in detail.

→ Indeed, this observation is only true when considering the same model and boundary conditions (except for the SST of the HadCM3L), but is not correct when considering the different boundary conditions (i.e Eocene vs Cretaceous for the ECHAM5 and CCSM3). We also have different meridional gradients for the same model/boundary conditions but with different model parametrization (e.g. altered cloud physics). We made the correction in the manuscript:
*"However, when comparing different studies with the same model (Cretaceous vs Eocene for ECHAM5 and CCSM3) it is not the case, indicating the major role of boundary conditions in defining the latitudinal temperature gradient. For instance, the South Hemisphere gradient obtained for the Eocene with the ECHAM5 model is always lower than those obtained for the Cretaceous with the same model, regardless of the $pCO_2$ value (See Fig. 11 and Supplementary Data)."*

Page 16, line 441: The title of the subsection is a bit misleading, since not only Cretaceous studies are discussed (also e.g. Eocene).

→ Modified title: 4.2 PRIMARY CLIMATE CONTROLS

Page 16, lines 446-448: 2000 years are not very long for equilibrium climate sensitivity simulations, and the 4x$CO_2$ simulations do still show a significant trend at the end (SST cooling by about 1K/thousand years; Fig. 1); this should be pointed out here.

→ We have clarified this point:

- *Page 5, line 40: "The piControl simulation was run for 1800 years and the five others for 2000 years in order to reach a near-surface equilibrium (Fig.1)".*
- *Page 16 line 448: "The signal is notably due to a 9°C warming in response to the fourfold increase in $pCO_2$, which converts to an increase of 4.5°C for a doubling of $pCO_2$ (assuming that the response is linear). This sensitivity agrees with the higher end of the range of values in the investigations mentioned above. However, the sensitivity of IPSL-CM5A2 in our simulations could be slightly lower as the simulations are not completely equilibrated – see Figure 1)".*

Page 16, line 469: Please rephrase, "reduced gradient was amplified"?

→ Modified sentence : *It has been suggested that high latitude warming was amplified in deep time simulations by rising $CO_2$ via cloud and vegetation feedbacks (Otto-bliesner and Upchurch, 1997; Deconto et al., 2000) or by increasing ocean heat transport (Barron et al., 1995; Schmidt and Mysak, 1996; Brady et al., 1998), in particular when changing the paleogeography (Hotinski and Toggweiler, 2003), thus contributing to the flattening of the meridional SST gradient".*

Page 17, line 473: Please rephrase, "is the primary control" -> "is a primary control"; other similarly large effects may be missing in the model (given the model–proxy data mismatch).

→ Ok

Page 17, lines 484-488: What would be the probable effects of such a vegetation change, and what the implications for this study?

→ Modifications:
*"The presence of such a type of vegetation could change the albedo of continental regions, but also heat and water-vapor transfer by modified evapo-transpiration processes, thus leading to a warming amplification at high-altitudes and thus a reduced temperature gradient (Otto-bliesner and Upchurch, 1997; Hay et al., 2019). Based on these studies and on our results, we cannot exclude that this kind of high latitude vegetation can give more weight to the role of paleovegetation in reducing the temperature gradient".*

Page 18, lines 512-513: "Such modelling efforts would probably even more increase the equilibrium climate sensitivity, ..." This is interesting but speculative. Please delete or discuss in more detail / add references.

→ Deleted.

Page 18, data availability: Are the model source code and the applied boundary condition iles also available?

→ Yes, they are, we added the precisions to the manuscript.

Figure 1: Labels are too small.

Figure 2: Ticks and labels of oceanic area anomaly plot do not line up.

→ Modified.

Figure 4: Labels are too small. Fewer contour intervals might be better, also to identify the zero-line. Maybe this is just my printer, but I don't see white in the colorbar.

→ Labels and contour intervals modified. We also added in the figure legend that the white color (which is not in the colorbar) corresponds to areas where the anomaly is not significative regarding the student test.

Figure 5: Labels are way too small, especially in the lower panel. I do not know by hard what the usual cloud cover is at what pressure level. Plots of the total cloudiness from observations and from PI and maybe also 1x-NOICE would be helpful. Is the anomaly really plotted as the absolute difference in cloud cover, as suggested in the caption? That would indicate that the top of the simulated atmosphere is totally covered by clouds!?! Please also define in the text what is meant by high and low clouds.

→ We added in the figure legend and in the text, the level pressure for low-altitude cloudiness (>680 hPa) and high-altitude cloudiness (<440 hPa). The anomaly was not the absolute value but the change of cloudiness in % of the 1X-NOICE value. We changed the figure to be clearer and stay coherent with other anomaly figures, and plotted the absolute change.

Figure 6: Caption: "4xNI ... SOLAR-SOLAR" typo experiment name.

→ Modified.

Figure 9b+d: Instead of shifting the curves to the same equatorial temperatures, it might be better to plot the anomalies due to the individual boundary condition changes ($\_CO_2$, ...).

→ This could be an alternative, yes. However, we wanted to keep the shifted curve, as it is very visual to represent what is the 'gradient flattening", what would not be the case with anomalies.

Figure 10: The red dashed regression line is not visible in my copy.

→ We forgot to remove this from the figure legend. We finally didn't plot the regression line, not to overload the figure. The regression line is visible in the supplementary data file.

Figure 11: Labels are too small.

→ Modified.

**3 Language / typos**

There are numerous typos and little grammatical errors, as well as some unclear sentences; I would hence recommend copy editing. For example: Page 3, line 85: ...latest "work" are divided... "studies" instead?
Page 4, line 96: ...a set of simulation run... (missing plural s)
Page 9, lines 208-209: The whole surface is warmer... and which is generally larger over continents... (sentence structure)

Page 10, line 251: ...data ant temperature... (and)

→ Corrections done in the revised manuscript

## References


Barron, E. J., Fawcett, P. J., Peterson, W. H., Pollard, D. and Thompson, S. L.: A " simulation " of mid-Cretaceous climate Abstract . A series of general circulation model experiments W increased from present day ). By combining all three major variables levels of CO2 . Four times present-day • s W provided the best match to the this, , 10(5), 953–962, 1995.

Berner, R. A.: GEOCARBSULF: A combined model for Phanerozoic atmospheric O2 and CO2, Geochim. Cosmochim. Acta, 70(23 SPEC. ISS.), 5653–5664, doi:10.1016/j.gca.2005.11.032, 2006.

Bice, K. L., Birgel, D., Meyers, P. A., Dahl, K. A., Hinrichs, K. U. and Norris, R. D.: A multiple proxy and model study of Cretaceous upper ocean temperatures and atmospheric CO2 concentrations, Paleoceanography, 21(2), 1–17, doi:10.1029/2005PA001203, 2006.

Brady, E. C., Deconto, R. M. and Thompson, S. L.: Deep Water Formation and Poleward Ocean Heat Transport in the Warm Climate Extreme of the Cretaceous ( 80 Ma ) evidence, , 25(22), 4205–4208, 1998.

Deconto, R. M., Brady, E. C., Bergengren, J. and Hay, W. W.: Late Cretaceous climate, vegetation, and ocean interactions, Warm Clim. Earth Hist., 275–296, doi:10.1017/cbo9780511564512.010, 2000.

Goldner, A., Herold, N. and Huber, M.: Antarctic glaciation caused ocean circulation changes at the Eocene-Oligocene transition, Nature, 511(7511), 574–577, doi:10.1038/nature13597, 2014.

Hay, W. W., DeConto, R. M., de Boer, P., Flögel, S., Song, Y. and Stepashko, A.: Possible solutions to several enigmas of Cretaceous climate, Springer Berlin Heidelberg., 2019.

Hotinski, R. M. and Toggweiler, J. R.: Impact of a Tethyan circumglobal passage on ocean heat transport and “equable” climates, Paleoceanography, 18(1), n/a-n/a, doi:10.1029/2001PA000730, 2003.

Kennedy-asser, A. T., Lunt, D. J., Valdes, P. J., Ladant, J., Frieling, J. and Lauretano, V.: Changes in the high latitude Southern Hemisphere through the Eocene-Oligocene Transition : a model-data comparison, Clim. Past, (September), 1–26, doi:https://doi.org/10.5194/cp-2019-112, 2019.

Kennedy, A. T., Farnsworth, A., Lunt, D. J., Lear, C. H. and Markwick, P. J.: Atmospheric and oceanic impacts of Antarctic glaciation across the Eocene-Oligocene transition, Philos. Trans. R. Soc. A Math. Phys. Eng. Sci., 373(2054), doi:10.1098/rsta.2014.0419, 2015.

Knorr, G. and Lohmann, G.: Climate warming during antarctic ice sheet expansion at the middle miocene transition, Nat. Geosci., 7(5), 376–381, doi:10.1038/ngeo2119, 2014.

Krinner, G., Viovy, N., de Noblet-Ducoudré, N., Ogée, J., Polcher, J., Friedlingstein, P., Ciais, P., Sitch, S. and Prentice, I. C.: A dynamic global vegetation model for studies of the coupled atmosphere-biosphere system, Global Biogeochem. Cycles, 19(1), 1–33, doi:10.1029/2003GB002199, 2005.

Ladant, J. B. and Donnadieu, Y.: Palaeogeographic regulation of glacial events during the Cretaceous supergreenhouse, Nat. Commun., 7(April 2017), 1–9, doi:10.1038/ncomms12771, 2016.

Lunt, D. J., Haywood, A. M., Schmidt, G. A., Salzmann, U., Valdes, P. J., Dowsett, H. J. and Loptson, C. A.: On the causes of mid-Pliocene warmth and polar amplification, Earth Planet. Sci. Lett., 321–322,

128–138, doi:10.1016/j.epsl.2011.12.042, 2012.
Lunt, D. J., Huber, M., Anagnostou, E., Baatsen, M. L. J., Caballero, R., DeConto, R., Dijkstra, H. A., Donnadieu, Y., Evans, D., Feng, R., Foster, G. L., Gasson, E., Von Der Heydt, A. S., Hollis, C. J., Inglis, G. N., Jones, S. M., Kiehl, J., Turner, S. K., Korty, R. L., Kozdon, R., Krishnan, S., Ladant, J. B., Langebroek, P., Lear, C. H., LeGrande, A. N., Littler, K., Markwick, P., Otto-Bliesner, B., Pearson, P., Poulsen, C. J., Salzmann, U., Shields, C., Snell, K., Stärz, M., Super, J., Tabor, C., Tierney, J. E., Tourte, G. J. L., Tripati, A., Upchurch, G. R., Wade, B. S., Wing, S. L., Winguth, A. M. E., Wright, N. M., Zachos, J. C. and Zeebe, R. E.: The DeepMIP contribution to PMIP4: Experimental design for model simulations of the EECO, PETM, and pre-PETM (version 1.0), Geosci. Model Dev., 10(2), 889–901, doi:10.5194/gmd-10-889-2017, 2017.
Maffre, P., Ladant, J. B., Donnadieu, Y., Sepulchre, P. and Goddéris, Y.: The influence of orography on modern ocean circulation, Clim. Dyn., 50(3–4), 1277–1289, doi:10.1007/s00382-017-3683-0, 2018.
Monteiro, F. M., Pancost, R. D., Ridgwell, A. and Donnadieu, Y.: Nutrients as the dominant control on the spread of anoxia and euxinia across the Cenomanian-Turonian oceanic anoxic event (OAE2): Model-data comparison, Paleoceanography, 27(4), 1–17, doi:10.1029/2012PA002351, 2012.
Otto-bliesner, B. L. and Upchurch, G. R.: the Late Cretaceous period, , 385127(February), 18–21, 1997.
Poulsen, C. J., Barron, E. J., Arthur, M. A. and Peterson, W. H.: Response of the mid-Cretaceous global oceanic circulation to tectonic and CO<inf>2</inf> forcings, Paleoceanography, 16(6), 576–592, doi:10.1029/2000PA000579, 2001.
Poulsen, C. J., Pollard, D. and White, T. S.: General circulation model simulation of the δ18O content of continental precipitation in the middle Cretaceous: A model-proxy comparison, Geology, 35(3), 199–202, doi:10.1130/G23343A.1, 2007.
Schmidt, G. A. and Mysak, L. A.: Can increased poleward oceanic heat flux explain the warm Cretaceous climate?, Paleoceanography, 11(5), 579–593, doi:10.1029/96PA01851, 1996.
Sepulchre, P., Caubel, A., Ladant, J., Bopp, L., Boucher, O., Braconnot, P., Brockmann, P., Cozic, A., Donnadieu, Y., Estella-perez, V., Ethé, C., Fluteau, F., Foujols, M., Gastineau, G., Ghattas, J., Hauglustaine, D., Hourdin, F., Kageyama, M., Khodri, M., Marti, O., Meurdesoif, Y., Mignot, J., Sarr, A., Servonnat, J., Swingedouw, D., Szopa, S. and Tardif, D.: IPSL-CM5A2 . An Earth System Model designed for multi-millennial climate simulations, , (December), 2019.
Tabor, C. R., Poulsen, C. J., Lunt, D. J., Rosenbloom, N. A., Otto-Bliesner, B. L., Markwick, P. J., Brady, E. C., Farnsworth, A. and Feng, R.: The cause of Late Cretaceous cooling: A multimodel-proxy comparison, Geology, 44(11), 963–966, doi:10.1130/G38363.1, 2016.
Upchurch, G. R., Kiehl, J., Shields, C., Scherer, J. and Scotese, C.: Latitudinal temperature gradients and high-latitude temperatures during the latest Cretaceous: Congruence of geologic data and climate models, Geology, 43(8), 683–686, doi:10.1130/G36802.1, 2015.

## Response to comments by Alexander Farnsworth (referee #2)

### 1 General comments

Why should the Cenomanian-Turonian thermal maximum be of more relevance than that of the PETM, MECO, etc. to the future. Worthwhile to flesh out why this particular time period is deemed important.

→ We did not mean to imply that the Cenomanian-Turonian thermal maximum was of more relevance to the future than other greenhouse intervals of the deep-time past. However, the CT thermal maximum can be of particular interest (as can be the PETM) in that it is a time interval with elevated atmospheric $CO_2$ levels, probably similar or even higher than those expected in the future under a business-as-usual carbon emission scenario. In this manuscript, we present a CT simulation, which has been performed as part of a greater project on OAE2, but we note that Early Eocene and PETM simulations have also been performed by the same group and are part of the DeepMIP project (Lunt et al., Clim. Past 2020, in review). We have clarified the text as follows:

*"The Cretaceous period is of particular interest to understand drivers of past greenhouse climates because intervals of prolonged global warmth (O'Brien et al. 2017, Huber et al. 2018) and elevated atmospheric $CO_2$ levels (Wang et al., 2014), possibly similar to future levels, have been documented in the proxy record. The thermal maximum of the Cenomanian-Turonian (CT) interval (94 Ma) represents the acme of Cretaceous warmth, during which occurred one of the most important carbon cycle perturbation of the Phanerozoic, the oceanic anoxic event 2 (OAE2). Valuable understanding can hence be drawn from investigations of the mechanisms responsible for the CT thermal maximum and carbon cycle perturbation."*

There will also be non-linear feedbacks that cannot be deconvolved with the current methodology. I.e. The proportion of landmass at different latitudes between the pre-industrial and Cretaceous at Preindustrial CO2 levels (and topographic height differences) will have a dissimilar impact on the vegetation response and in turn the warming response from increased CO2.

→ We agree and note that referee #1 also raised this point. We agree that repeating the experiments with a different sequence of changes would be desirable to fully assess the shortcomings of the linear factorization method. It indeed has been suggested that a different sequence of boundary condition changes would probably give different results (Lunt et al., 2012). However, these additional experiments using the IPSL-CM5A2 earth system model require a computational cost that we cannot afford.
We have added the following discussion about linear factorization in the revised manuscript:

*"The choice of applying a linear factorization approach was made for problems of computing time and cost. Changing the sequence of changes or applying a symmetrical factorization as in Lunt et al (2012) would require too many supplementary simulations. However, such a method is very dependent on the sequence of changes, and results would be probably different if boundary conditions were change in a different order* (Lunt et al., 2012)*".*

I did sometimes get a bit confused with the methodology section. It was sometimes hard to see what models were initialised with what initial conditions. How were some of the boundary conditions treated. i.e. what were the actual albedo prescribed? Was the vegetation uniformly applied even to mountain regions where it may not

grow? Might be worth being a bit more concise in describing them individual boundary conditions and how they were implemented for clarity and reproducibility.

→ The description of boundary conditions will be reorganized to be clearer.

**2 Minor points.**

Page 5 – Line 40. It looks like only the 1X-NOICE is in equilibrium in the deep ocean. The other four still appear to be trending. I think for clarity this should be stated or changed to "near-surface equilibrium". I certainly sympathize as some of my own simulations can take up to 10,000 model years to reach equilibrium. However, I do not think this will change the overall results, but for clarity it should not be stated as complete equilibrium. Gregory plots may also be another useful diagnostic to see if you have an energy imbalance otherwise.

→ Simulations are indeed not perfectly equilibrated and we have clarified the text:

*Page 5, line 40: "The piControl simulation was run for 1800 years and the five others for 2000 years in order to reach a near-surface equilibrium (Fig.1)".*

Ice sheet removal impact. I agree with your assessment of the regional impact, however it might also be that you get a pseudo ice sheet in the 1X-NOICE simulation with perennial snow cover over the soil surface, just a low elevation one. I suspect this is the case as in the 4X-NOICE you get a much large response in the change in surface and planetary albedo. Did you ever run a 4xCO2 experiment with ice sheets in the pre-industrial to see the relative impact of just the CO2?

→ Unfortunately, we did not perform a 4X $CO_2$ simulation with prescribed preindustrial ice sheets. Indeed, we have a snow cover in the 1X-NOICE, but it is also the case in the 4X-NOICE, and the snow cover is even larger over the Antarctic in the 4X-NOICE than in the 1X-NOICE because of a larger amount of precipitations.

The large decrease of surface albedo seen between the 1X-NOICE and the 4X-NOICE is due to the decrease of sea ice. We will add figures of surface albedo in the supplementary figures.

*Snow mass annual average (kg/m2) over the Antarctic for1X-NOICE and 4X-NOICE simulations and corresponding anomaly.*

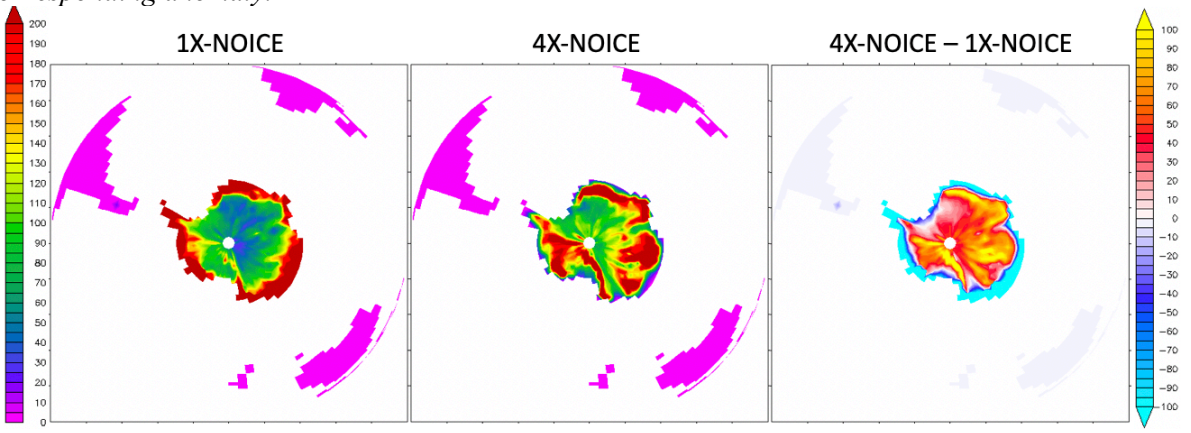

*Surface albedo average (%) in the Austral ocean for1X-NOICE and 4X-NOICE simulations and corresponding anomaly.*

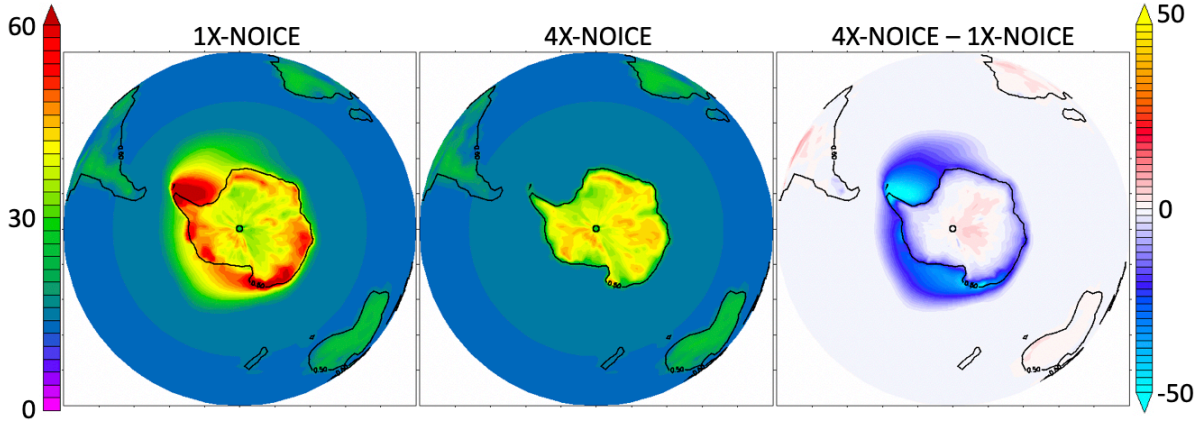


*Surface albedo annual average (%) in the Arctic for1X-NOICE and 4X-NOICE simulations and corresponding anomaly.*

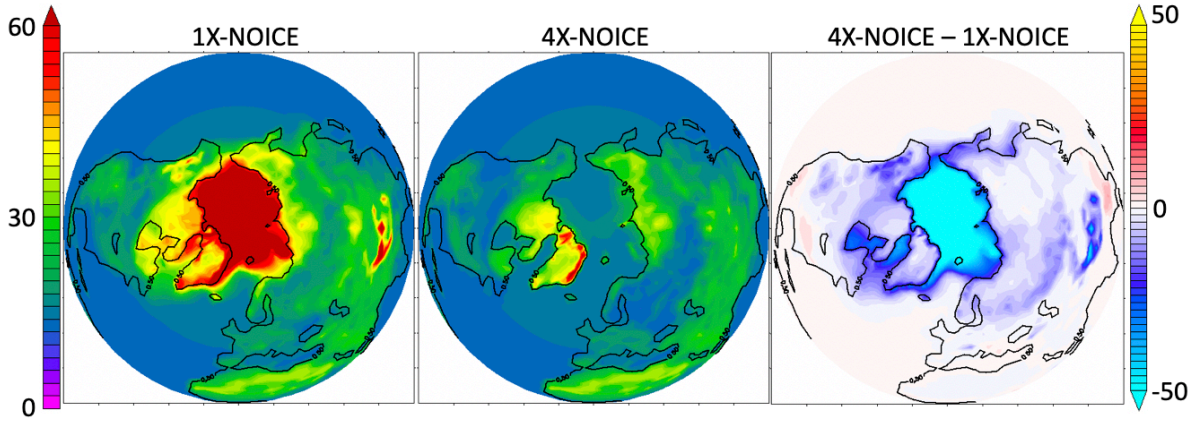


*Sea-ice annual average (%) in the Austral ocean for1X-NOICE and 4X-NOICE simulations and corresponding anomaly.*

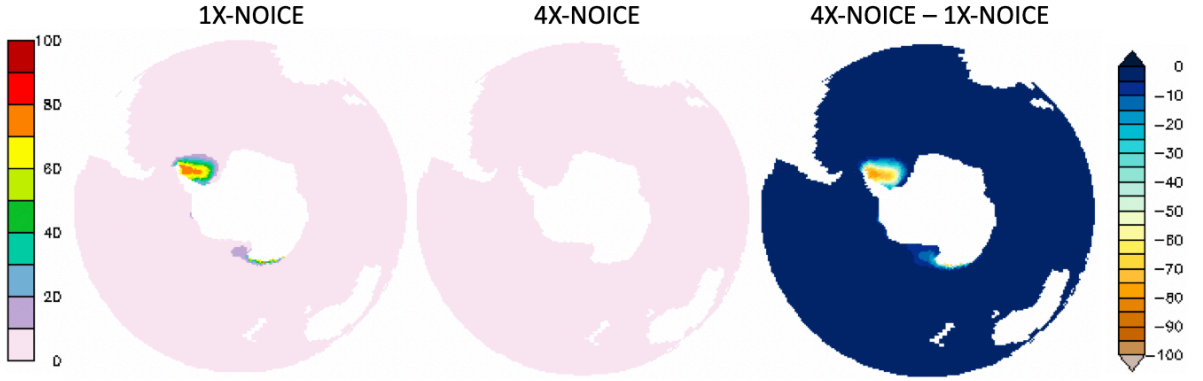


*Sea-ice annual average (%) in the Arctic for1X-NOICE and 4X-NOICE simulations and corresponding anomaly.*

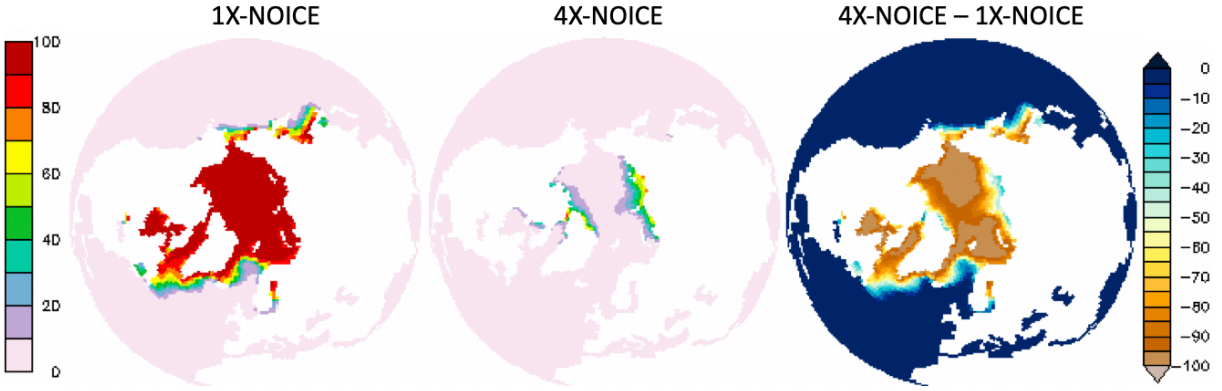


Do you see any change in ocean circulation patterns from removal of the ice sheet and increased CO2 in the preindustrial?

→ The global meridional stream function keeps the same structure when removing ice sheets or increasing CO2 in the preindustrial. However, the intensity of ocean circulation changes. In the simulation without ice sheets, NADW is slightly weaker whereas AABW is slightly stronger relative to the preindustrial. The 4x CO2 simulation predicts stronger AABW and NADW with a shallowing of the NADW.

*Global meridional stream function (Sv) for piControl, 1X-NOICE and 4X-NOICE simulations. Positive values (red) indicate a clockwise circulation and negative values (blue) an anticlockwise circulation.*

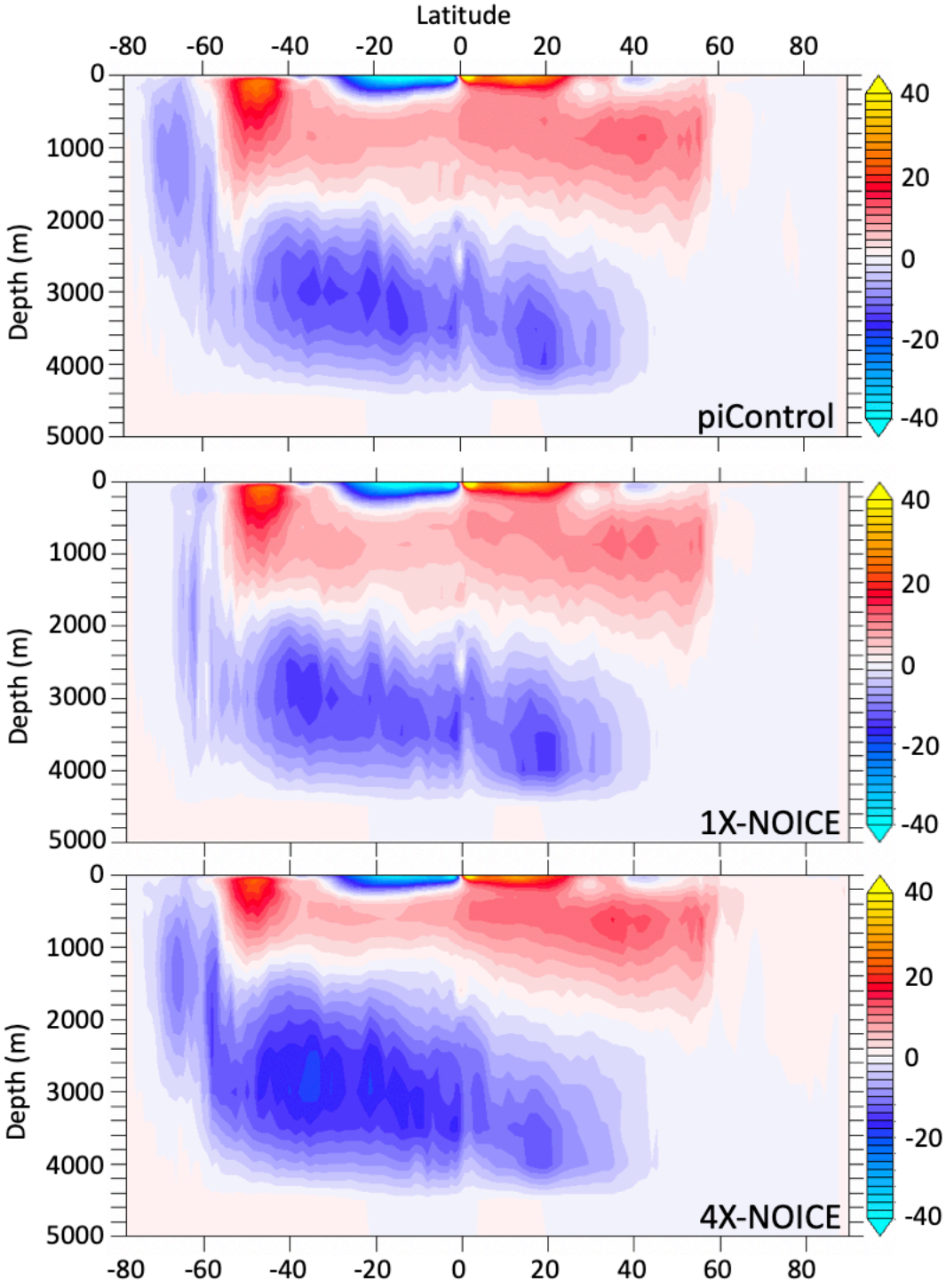
Latitude
-80
-60
-40
-20
0
20
40
60
80
Depth (m)
0
1000
2000
3000
4000
5000
40
20
0
-20
-40
piControl
1X-NOICE
4X-NOICE

We can see also some local changes of surface circulation around the Antarctic when removing the polar ice cap, that seems to be related to changes in winds. These changes are probably driving the cooling patch that we can see on fig. 4b, that corresponds to a local increase of sea ice.
We didn't want to detail this in the manuscript as it is regional changes.

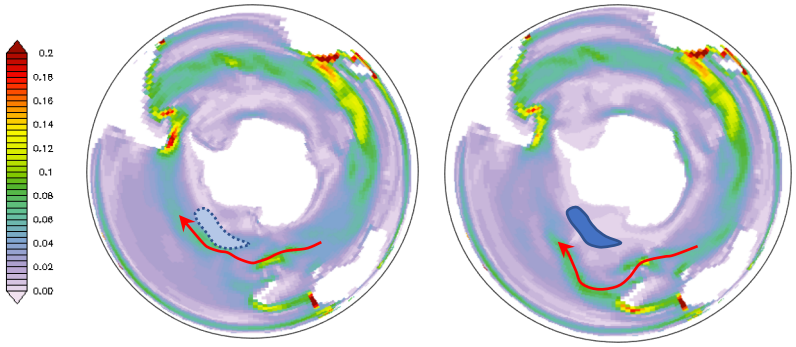


*Currents velocity for piControl (left) and 1X-NOICE (right) simulations. The red arrow shows the ACC position. The blue box shows the position of the sea ice increase (=cooling area).*

661 **3**

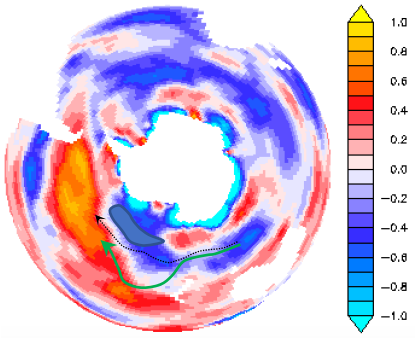


*Sea surface wind speed anomaly during winter (1X-NOICE-piControl). The polar ice cap removal causes a displacement of winds and thus ACC to the North, which allows an increase of sea ice in the 1X-NOICE simulation. Blue box: Sea ice anomaly, Black arrow: ACC position for the piControl simulation, Green arrow: ACC position for the 1X-NOICE simulation (after polar cap removal).*

**Minor comments.**

Page 1 & 2 – Line 17 & 33. 'period' not "era"

→ Modified.

I think it is worthwhile to define what you mean by 'high' and 'low' latitudes as you often see different values purported in different studies for clarity.

→ Done: "*high-latitudes (> 60° of latitude)*"; "*low-latitudes (< 30° of latitude)*"

Throughout – put references in chronological order.
Page 2, Line 60. Define "P.A.L." here. This is the first instance in the ms rather than on page 6- line 50.
Page 3 – Line 79. Change sentence to "the primary driver of Cretaceous climate has been suggested".
Page 3 – Line 83. Delete erroneous "s".

→ Done.

Page 4 – Line 96. Probably more accurate to say "We performed six simulations using both Pre industrial and Late Cretaceous boundary conditions where we incrementally modify the Pre-industrial boundary conditions to that of the Late Cretaceous for: : :: : :1,2,3,4".

→ Thank you for this suggestion. The sentence was rephrased as: "*We performed six simulations, using both preindustrial and Late Cretaceous boundary conditions where we incrementally modify the preindustrial boundary conditions to that of the Late Cretaceous for the following…".*

Page 4. Although stated that IPSL-CM5A2 has been used for contemporary and future climate simulations it would be worth adding a line that states how well the model performs in simulating a modern-day climate.

→ The performances of the IPSL-CM5A2 are fully described in (Sepulchre et al., 2019), we added the reference to the manuscript: *"Building on technical developments, IPSL-CM5A2 provides enhanced computing performances compared to IPSL-CM5A-LR, allowing thousand-years long integrations required for deep-time paleoclimate applications or long-term future projections (Sepulchre et al., 2019). IPSL-CM5A2 reasonably simulates modern-day and historical climates (despite some biases in the tropics), whose complete description and evaluation can be found in Sepulchre et al., 2019."*

Page 5 – Line 20. Repetition of "long" in the sentence. Remove one of them.
Page 5 – Line 37. "retreat" to retreat. But I think 'removed' would be more accurate.

→ Done.

Page 6 – Line 53. Is that from the 4X-NOICE simulation?

→ We will give more precisions in the manuscript (see also reponse to comment from reviewer #1): we have adapted the Lunt et al., 2017 formulation has the Cenomanian-Turonian ocean was warmer (see also Sepulchre et al., 2019) :

If depth ≤ 1000 m :

$$T = 10 + \left(\frac{1000 - depth}{1000}\right) * 25\cos(latitude)$$

if depth > 1000 m :

T = 10

Page 6 – Line 218-222. Did you look at atmospheric stability arguments in relation to this?

→ Indeed, we should look at atmospheric stability to explain the observations made in relation to these processes that are quite complex. We would need to go into details regarding the changes in water content, relative/specific/absolute humidity as well as atmospheric dynamics to explain the observed changes. We do not want to go into such details in the manuscript which is already long and which not specifically focus on the impact of a CO2 increase, so we finally decided to remove this paragraph.

Page 6 – Line 223. Do you mean greater season ice melt or there being less sea ice area in the 4X-NOICE compared to the 1X-NOICE simulation?

→ Less sea ice in the 4X-NOICE: *"The sea level pressure decrease is possibly a feedback driven by reduced sea ice cover and associated higher temperatures."*

Page 12 – Section 3.5.1. The percentage change adds to 99%. Rounding error?

→ The 30% was actually a 31%, but we finally decided to remove the percentages as it was confusing and to keep only raw values (see also comments from reviewer #1).

Page 12 –Line 321-324: There does not appear to be any change in the N.Hem SST gradients (0.45/lat). Any idea why? You attribute the Greenland ice sheet/sea ice for less sensitivity in the atmospheric gradient of the N.Hem. Something similar here?

→ Indeed, by calculating the gradient with the temperature value at 80°N it seems that there is no flattening. However, if we look at the figure 9b, we can see that the gradient is flatter until 70° of latitude North and is very steep beyond. It light be because the arctic ocean is very isolated due to the paleogeographic configuration, which doesn't allow heat transport beyond 80°N.

Page 14 – Line 370. Do you mean that you used the Tabor, et al. dataset and adding more data points

→ Yes, we clarified it : *"Our SST data compilation is modified from Tabor et al (2016), with additional data from more recent studies (see Supplementary data)."*

Page 14 –Line 388. Only if you suggest there is a seasonal proxy bias. This is mentioned later on, but might be worth a few ref's that show there are seasonal bias in some proxies.

→ Done: *"This congruence would imply that a seasonal bias may exist in temperatures reconstructed from proxies, which is suggested in previous studies (Sluijs et al., 2006; Hollis et al., 2012; Huber, 2012)."*

Page 16 – Line 448. Do you mean 'more complex' rather than "large"?

→ Modified sentences: *"The signal is notably due to a 9°C warming in response to the fourfold increase in $pCO_2$, which converts to an increase of 4.5°C for a doubling of $pCO_2$ (assuming that the response is linear). This sensitivity agrees with the higher end of the range of values in the investigations mentioned above. However, the sensitivity of IPSL-CM5A2 in our simulations could be slightly lower as the simulations are not completely equilibrated – see Figure 1)."*

Page 17 – Line 480. "cloud" not "clouds".

→ Modified.

Page 17 – Conclusions section. This is a tad bit repetitive of the results/discussion. Perhaps broaden this out with respect to the discussion in your introduction.

→ We will arrange the conclusions to be less repetitive and to fit with raised questions in the introduction

Figure 1, 5,6, 8, 9, 11 Captions. Add 'mean annual' to caption.

→ Done.

Figure 2. Is that the model resolution geographies?

→ Bathymetry was shown at the model resolution but not the topography that is shown with a bilinear interpolation. We will change the figure to show the model resolution for the topography also.

Figure 11b. Appears to be some modelling studies missing? E.g. HadCM3L 2xCO2 data point and others. Or was I interpreting this wrongly? Quite possible!

→ Indeed, some points were missing! We added them.

## References


Hollis, C. J., Taylor, K. W. R., Handley, L., Pancost, R. D., Huber, M., Creech, J. B., Hines, B. R., Crouch, E. M., Morgans, H. E. G., Crampton, J. S., Gibbs, S., Pearson, P. N. and Zachos, J. C.: Early Paleogene temperature history of the Southwest Pacific Ocean : Reconciling proxies and models, Earth Planet. Sci. Lett., 349–350, 53–66, doi:10.1016/j.epsl.2012.06.024, 2012.

Huber, M.: Progress in Greenhouse Climate Modeling, Paleontol. Soc. Pap., 18, 213–262, doi:10.1017/s108933260000262x, 2012.

Lunt, D. J., Haywood, A. M., Schmidt, G. A., Salzmann, U., Valdes, P. J., Dowsett, H. J. and Loptson, C. A.: On the causes of mid-Pliocene warmth and polar amplification, Earth Planet. Sci. Lett., 321–322, 128–138, doi:10.1016/j.epsl.2011.12.042, 2012.

Lunt, D. J., Huber, M., Anagnostou, E., Baatsen, M. L. J., Caballero, R., DeConto, R., Dijkstra, H. A., Donnadieu, Y., Evans, D., Feng, R., Foster, G. L., Gasson, E., Von Der Heydt, A. S., Hollis, C. J., Inglis, G. N., Jones, S. M., Kiehl, J., Turner, S. K., Korty, R. L., Kozdon, R., Krishnan, S., Ladant, J. B., Langebroek, P., Lear, C. H., LeGrande, A. N., Littler, K., Markwick, P., Otto-Bliesner, B., Pearson, P., Poulsen, C. J., Salzmann, U., Shields, C., Snell, K., Stärz, M., Super, J., Tabor, C., Tierney, J. E., Tourte, G. J. L., Tripati, A., Upchurch, G. R., Wade, B. S., Wing, S. L., Winguth, A. M. E., Wright, N. M., Zachos, J. C. and Zeebe, R. E.: The DeepMIP contribution to PMIP4: Experimental design for model simulations of the EECO, PETM, and pre-PETM (version 1.0), Geosci. Model Dev., 10(2), 889–901, doi:10.5194/gmd-10-889-2017, 2017.

Sepulchre, P., Caubel, A., Ladant, J., Bopp, L., Boucher, O., Braconnot, P., Brockmann, P., Cozic, A., Donnadieu, Y., Estella-perez, V., Ethé, C., Fluteau, F., Foujols, M., Gastineau, G., Ghattas, J., Hauglustaine, D., Hourdin, F., Kageyama, M., Khodri, M., Marti, O., Meurdesoif, Y., Mignot, J., Sarr, A., Servonnat, J., Swingedouw, D., Szopa, S. and Tardif, D.: IPSL-CM5A2 . An Earth System Model designed for multi-millennial climate simulations, , (December), 2019.

Sluijs, A., Schouten, S., Pagani, M., Woltering, M. and Brinkhuis, H.: Subtropical Arctic Ocean temperatures during the Palaeocene / Eocene thermal maximum, , (May 2014), doi:10.1038/nature04668, 2006.

Tabor, C. R., Poulsen, C. J., Lunt, D. J., Rosenbloom, N. A., Otto-Bliesner, B. L., Markwick, P. J., Brady, E. C., Farnsworth, A. and Feng, R.: The cause of Late Cretaceous cooling: A multimodel-proxy comparison, Geology, 44(11), 963–966, doi:10.1130/G38363.1, 2016.

Wang, Y., Huang, C., Sun, B., Quan, C., Wu, J. and Lin, Z.: Paleo-CO2 variation trends and the Cretaceous greenhouse climate, Earth-Science Rev., 129, 136–147, doi:10.1016/j.earscirev.2013.11.001, 2014.

# Stripping back the Modern to reveal the Cenomanian-Turonian climate and temperature gradient underneath

Marie Laugié[1], Yannick Donnadieu[1], Jean-Baptiste Ladant[2], Mattias Green[3], Laurent Bopp[4,5] and François Raisson[6].

[1]Aix Marseille Univ, CNRS, IRD, INRA, Coll. France, CEREGE, Aix-en-Provence, France
[2]Department of Earth and Environmental Sciences, University of Michigan, Ann Arbor, MI, USA
[3]School of Ocean Sciences, Bangor University, Menai Bridge, UK
[4]Ecole Normale Supérieure (ENS Paris) - Département des Géosciences - France
[5]Laboratoire de Météorologie Dynamique (UMR 8539) (LMD) - Université Pierre et Marie Curie - Paris 6, Institut national des sciences de l'Univers, École Polytechnique, École des Ponts ParisTech, Centre National de la Recherche Scientifique : UMR8539, École Normale Supérieure - Paris - France
[6]Total EP – R&D Frontier Exploration - France

## ABSTRACT

During past geological times, the Earth experienced several intervals of global warmth, but their driving factors remain equivocal. A careful appraisal of the main processes controlling past warm events is essential to inform future climates and ultimately provide decision makers with a clear understanding of the processes at play in a warmer world. In this context, intervals of greenhouse climates, such as the thermal maximum of the Cenomanian-Turonian (~94 Ma) during the Cretaceous period, are of particular interest. Here we use the IPSL-CM5A2 Earth System Model to unravel the forcing parameters of the Cenomanian-Turonian greenhouse climate. We perform six simulations with an incremental change in five major boundary conditions in order to isolate their respective role on climate change between the Cenomanian-Turonian and the preindustrial. Starting with a preindustrial simulation, we implement the following changes in boundary conditions: (1) the absence of polar ice sheets, (2) the increase in atmospheric $pCO_2$ to 1120 ppm, (3) the change of vegetation and soil parameters, (4) the 1% decrease in the Cenomanian-Turonian value of the solar constant and (5) the Cenomanian-Turonian paleogeography. Between the preindustrial simulation and the Cretaceous simulation, the model simulates a global warming of more than 11°C. Most of this warming is driven by the increase in atmospheric $pCO_2$ to 1120 ppm. Paleogeographic changes represent the second major contributor to global warming, whereas the reduction in the solar constant counteracts most of geographically-driven warming. We further demonstrate that the implementation of Cenomanian-Turonian boundary conditions flattens meridional temperature gradients compared to the preindustrial simulation. Interestingly, we show that paleogeography is the major driver of the flattening in the low- to mid-latitudes, whereas $pCO_2$ rise and polar ice sheet retreat dominate the high-latitude response.

# 1. INTRODUCTION

The Cretaceous period is of particular interest to understand drivers of past greenhouse climates because intervals of prolonged global warmth (O'Brien et al. 2017, Huber et al. 2018) and elevated atmospheric $CO_2$ levels (Wang et al., 2014), possibly similar to future levels, have been documented in the proxy record. The thermal maximum of the Cenomanian-Turonian (CT) interval (94 Ma) represents the acme of Cretaceous warmth, during which one of the most important carbon cycle perturbation of the Phanerozoic occurred: the oceanic anoxic event 2 (OAE2; Jenkyns, 2010; Huber et al., 2018). Valuable understanding of what controls large-scale climate processes can hence be drawn from investigations of the mechanisms responsible for the CT thermal maximum and carbon cycle perturbation.

Proxy-based reconstructions and model simulations of sea-surface temperatures (SST) for the CT reveal that during OAE2 the equatorial Atlantic was 4-6° warmer than today (Norris et al., 2002; Bice et al., 2006; Pucéat et al., 2007; Tabor et al., 2016), and possibly even warmer than that (6-9° - Forster et al., 2007). This short and abrupt episode of major climatic, oceanographic, and global carbon cycle perturbations occurred at the CT Boundary and was superimposed on a long period of global warmth (Jenkyns, 2010). The high latitudes were also much warmer than today (Herman and Spicer, 2010; Spicer and Herman, 2010), as was the abyssal ocean which experienced bottom temperatures reaching up to 20°C during the CT (Huber et al., 2002; Littler et al., 2011; Friedrich et al., 2012). Paleobotanical studies suggest that the atmosphere was also much warmer (Herman and Spicer, 1996), with high-latitude temperatures up to 17°C higher than today (Herman and Spicer, 2010) and possibly reaching annual means of 10-12°C in Antarctica (Huber et al., 1999).

The steepness of the equator-to-pole gradient is still a matter of debate, in particular because of inconsistencies between data and models as the latter usually predict steeper gradients than those reconstructed from proxy data (Barron, 1993; Huber et al., 1995; Heinemann et al., 2009; Tabor et al., 2016). Models and data generally agree, however, that Cretaceous sea-surface temperature (SST) gradients were reduced compared to today (Sellwood et al., 1994; Huber et al., 1995; Jenkyns et al., 2004; O'Brien et al., 2017; Robinson et al., 2019).

The main factor generally considered responsible for the Cretaceous global warm climate is the higher atmospheric $CO_2$ concentration (Barron et al., 1995; Crowley and Berner, 2001; Royer et al., 2007; Wang et al., 2014; Foster et al., 2017). This has been determined by proxy-data reconstructions of the Cretaceous $pCO_2$ using various techniques, including analysis of paleosols $\delta^{13}C$ (Sandler and Harlavan, 2006; Leier et al., 2009; Hong and

Lee, 2012), liverworts $\delta^{13}C$ (Fletcher et al., 2006) or phytane $\delta^{13}C$ (Damsté et al., 2008; Van Bentum et al., 2012) and leaf stomata analysis (Barclay et al., 2010; Mays et al., 2015; Retallack and Conde, 2020). Modelling studies have also focused on estimating Cretaceous atmospheric $CO_2$ levels (Barron et al., 1995; Poulsen et al., 2001, 2007; Berner, 2006; Bice et al., 2006; Monteiro et al., 2012) in an attempt to refine the large spread in values inferred from proxy data (from less than 900 ppm to over 5000 ppm). The typical atmospheric $pCO_2$ concentration resulting from these studies for the CT averages around a long-term value of 1120 ppm (Barron et al., 1995; Bice and Norris, 2003; Royer, 2013; Wang et al., 2014), e.g., four times the preindustrial value (280 ppm = 1 P.A.L : "Preindustrial Atmospheric Level"). Atmospheric $pCO_2$ levels are, however, known to vary on shorter timescales during the period, in particular during OAE2. It has indeed been suggested that this event may have been caused by a large increase in atmospheric $pCO_2$ concentration, possibly reaching 2000 ppm or even higher, because of volcanic activity in large igneous provinces (Kerr and Kerr, 1998; Turgeon and Creaser, 2008; Jenkyns, 2010). The proxy records suggest that the $pCO_2$ levels may have dropped down to 900 ppm after carbon sequestration into organic-rich marine sediments (Van Bentum et al., 2012).

Paleogeography is also considered as a major driver of climate change through geological times (Crowley et al., 1986; Gyllenhaal et al., 1991; Goddéris et al., 2014; Lunt et al., 2016). Several processes linked to paleogeographic changes have been shown to impact Cretaceous climates. These processes include albedo and evapotranspiration feedbacks from paleovegetation (Otto-bliesner and Upchurch, 1997), seasonality due to continental break-up or presence of epicontinental seas (Fluteau et al., 2007), atmospheric feedbacks due to water cycle modification (Donnadieu et al., 2006), Walker and Hadley cells changes after Gondwana break-up (Ohba and Ueda, 2011), or oceanic circulation changes due to gateways opening (Poulsen et al., 2001, 2003). Other potential controlling factors include the time-varying solar constant (Gough, 1981), whose impact on Cretaceous climate evolution was quantified by Lunt et al. (2016), and changes in the distribution of vegetation, which has been suggested to drive warming, especially in the high-latitudes with a temperature increase of up to 4°-10°C in polar regions (Otto-bliesner and Upchurch, 1997; Brady et al., 1998; Upchurch, 1998; Deconto et al., 2000; Hunter et al., 2013).

Despite all these studies, there is no established consensus on the relative importance of each of the controlling factors on the CT climate. In particular, the primary driver of the Cretaceous climate has been suggested to be either $pCO_2$ or paleogeography. Early studies suggested a negligible role of paleogeography on global climate compared to the high $CO_2$ concentration (Barron et al., 1995) whereas others suggested that $CO_2$

was not the primary control (Veizer et al., 2000) or that the impact of paleogeography on climate was as important as a doubling of $pCO_2$ (Crowley et al., 1986). More recent modeling studies have also suggested that paleogeographic changes could affect global climate (Poulsen et al., 2003; Donnadieu et al., 2006; Fluteau et al., 2007) but their impact remain debated (Ladant and Donnadieu, 2016; Lunt et al., 2016; Tabor et al., 2016). For example, the simulations of Lunt et al. (2016) support a key role of paleogeography at the regional rather than global scale, and show that the global paleogeographic signal is cancelled by an opposite trend due to changes in the solar constant. Tabor et al. (2016) also suggest important regional climatic impacts of paleogeography, but argue that $CO_2$ is the main driver of the Late Cretaceous climate evolution. In contrast, Ladant and Donnadieu (2016) find a large impact of paleogeography on the global mean Late Cretaceous temperatures; their signal is roughly comparable to a doubling of atmospheric $pCO_2$. Finally, the role of paleovegetation is also uncertain as some studies show a major role at high-latitude (Upchurch, 1998; Hunter et al., 2013), whereas a more recent study instead suggests limited impact at high latitudes (<2°C) with a cooling effect at low latitudes under high $pCO_2$ values (Zhou et al., 2012).

In this study, we investigate the forcing parameters of CT greenhouse climate by using a set of simulations run with the IPSL-CM5A2 Earth System Model. We perform six simulations, using both preindustrial and CT boundary conditions, where we incrementally modify the preindustrial boundary conditions to that of the CT. The changes are as follows: (1) the removal of polar ice sheets, (2) an increase in $pCO_2$ to 1120 ppm, (3) the change of vegetation and soil parameters, (4) a 1% reduction in the value of the solar constant, and (5) the implementation of Cenomanian-Turonian paleogeography. We particularly focus on processes driving warming or cooling of atmospheric surface temperatures after each change in boundary condition change to study the relative importance of each parameter in the CT to preindustrial climate change. We also investigate how the SST gradient responds to boundary condition changes to understand the evolution of its steepness between the CT and the preindustrial.

## 2. MODEL DESCRIPTION & EXPERIMENTAL DESIGN

### 2.1 IPSL-CM5A2 MODEL

IPSL-CM5A2 is an updated version of the IPSL-CM5A-LR earth system model developed at IPSL (Institut Pierre-Simon Laplace) within the CMIP5 framework (Dufresne et al., 2013). It is a fully-coupled Earth System Model, which simulates the interactions between atmosphere, ocean, sea ice, and land surface. The model

includes the marine carbon and other key biogeochemical cycles (C, P, N, O, Fe and Si - See Aumont et al., 2015). Its former version, IPSL-CM5A-LR, has a rich history of applications, including present-day and future climates (Aumont and Bopp, 2006; Swingedouw et al., 2017) as well as preindustrial (Gastineau et al., 2013) and paleoclimate studies (Kageyama et al., 2013; Contoux et al., 2015; Bopp et al., 2017; Tan et al., 2017; Sarr et al., 2019). It was also part of IPCC AR5 and CMIP5 projects (Dufresne et al., 2013). IPSL-CM5A-LR has also been used to explore links between marine productivity and climate (Bopp et al., 2013; Le Mézo et al., 2017; Ladant et al., 2018), vegetation and climate (Contoux et al., 2013; Woillez et al., 2014), and topography and climate (Maffre et al., 2018), but also the role of nutrients in the global carbon cycle (Tagliabue et al., 2010) or the variability of oceanic circulation and upwelling (Ortega et al., 2015; Swingedouw et al., 2015). Building on recent technical developments, IPSL-CM5A2 provides enhanced computing performances compared to IPSL-CM5A-LR, allowing thousand year-long integrations required for deep-time paleoclimate applications or long-term future projections (Sepulchre et al., 2019). It thus reasonably simulates modern-day and historical climates (despite some biases in the tropics), whose complete description and evaluation can be found in Sepulchre et al., 2019.

IPSL-CM5A2 is composed of the LMDZ atmospheric model (Hourdin et al., 2013), the ORCHIDEE land surface and vegetation model (including the continental hydrological cycle, vegetation, and carbon cycle; Krinner et al., 2005) and the NEMO ocean model (Madec, 2012), including the LIM2 sea-ice model (Fichefet and Maqueda, 1997) and the PISCES marine biogeochemistry model (Aumont et al., 2015). The OASIS coupler (Valcke et al., 2006) ensures a good synchronization of the different components and the XIOS input/output parallel library is used to read and write data. The LMDZ atmospheric component has a horizontal resolution of 96x95, (equivalent to 3.75° in longitude and 1.875° in latitude) and 39 uneven vertical levels. ORCHIDEE shares the same horizontal resolution whereas NEMO – the ocean component – has 31 uneven vertical levels (from 10 meters at the surface to 500 meters at the bottom), and a horizontal resolution of approximately 2°, enhanced to up to 0.5° in latitude in the tropics. NEMO uses the ORCA2.3 tripolar grid to overcome the North Pole singularity (Madec and Imbard, 1996).

## 2.2 EXPERIMENTAL DESIGN

Six simulations were performed for this study: one preindustrial control simulation, named piControl, and five simulations for which the boundary conditions were changed one at a time to progressively reconstruct the

CT climate (see Table 1 for details). The scenarios are called 1X-NOICE (with no polar ice sheets), 4X-NOICE (no polar ice sheets + pCO2 at 1120 ppm), 4X-NOICE-PFT-SOIL (previous changes + implementation of idealized Plant Functional Types (PFTs) and mean parameters for soil), 4X-NOICE-PFT-SOIL-SOLAR (previous changes + reduction of the solar constant) and 4X-CRETACEOUS (previous changes + CT paleogeography). The piControl simulation has been run for 1800 years and the five others for 2000 years in order to reach near-surface equilibrium (see Fig.1).

### 2.2.1 BOUNDARY CONDITIONS

As most evidence suggests the absence of permanent polar ice sheets during the CT (MacLeod et al., 2013; Ladant and Donnadieu, 2016; Huber et al., 2018), we remove polar ice sheets in our simulations (except in piControl) and we adjust topography to account for isostatic rebound resulting from the loss of the land ice covering Greenland and Antarctica (See Supplementary Figure 1). Ice sheets are replaced with brown bare soil and the river routing stays unchanged.

In the 4X simulations (i.e., all except piControl and 1X-NOICE), $pCO_2$ is fixed to 1120 ppm (4 P.A.L), a value reasonably close to the mean suggested by a recent compilation of CT $pCO_2$ reconstructions (Wang et al., 2014).

In the 4X-NOICE-PFT-SOIL simulation, the distribution of the 13 standard PFTs defined in ORCHIDEE is uniformly reassigned along latitudinal bands, based on a rough comparison with the preindustrial distribution of vegetation, in order to obtain a theoretical latitudinal distribution usable for any geological period. The list of PFTs and associated latitudinal distribution and fractions are described in Supplementary Table 1. Mean soil parameters, i.e., mean soil color and texture (rugosity), are calculated from preindustrial maps (Zobler, 1999; Wilson and Henderson-sellers, 2003) and uniformly prescribed on all continents. The impact of these idealized PFTs and mean parameters is discussed in the results.

The 4X-NOICE-PFT-SOIL-SOLAR simulation is initialized from the same conditions as 4X-NOICE-PFT-SOIL except that the solar constant is reduced to its CT value (Gough, 1981). We use here the value of 1353.36 $W/m^2$ (98.9% of the modern solar luminosity, calculated for an age of 90 My).

The 4X-CRETACEOUS simulation, finally, incorporates the previous modifications plus the implementation of the CT paleogeography. The land-sea configuration used here is that proposed by Sewall (2007), in which we have implemented the bathymetry from Müller (2008) (see Fig. 2). These bathymetric changes are done to represent deep oceanic topographic features, such as ridges, that are absent from the Sewall paleogeographic

configuration. In this simulation, the mean soil color and rugosity as well as the theoretical latitudinal PFTs distribution are adapted to the new land-sea mask and the river routing is recalculated from the new topography. We also modify the tidally driven mixing associated with dissipation o internal wave energy for the M2 and K1 tidal components from present day values (de Lavergne et al., 2019). The parameterization used for simulations with the modern geography follows Simmons et al. (2004), with refinements in the modern Indonesian Through Flow (ITF) region according to Koch-Larrouy et al. (2007). To create a Cenomanian-Turonian tidal dissipation forcing, we calculate an M2 tidal dissipation field using the Oregon State University Tidal Inversion System (OTIS, Egbert et al., 2004; Green and Huber, 2013). The M2 field is computed using our Cenomanian-Turonian bathymetry and an ocean stratification taken from an unpublished equilibrated Cenomanian-Turonian simulation realized with the IPSLCM5A2 with no M2 field. In the absence of any estimation for the CT, we prescribe the K1 tidal dissipation field to 0. In addition, the parameterization of Koch-Larrouy et al. (2007) is not used here because the ITF does not exist in the Cretaceous.

### 2.2.2 INITIAL CONDITIONS

The piControl and 1X-NOICE simulations are initialized with conditions from the Atmospheric Model Intercomparison Project (AMIP) which were constrained by realistic sea surface temperature (SST) and sea ice from 1979 to near present (Gates et al., 1999). In an attempt to reduce the integration time required to reach near-equilibrium, the initial conditions of simulations with 4 PAL are taken from warm idealized conditions (higher SST and no sea ice) adapted from those described in Lunt et al. (2017). The constant initial salinity field is set to 34.7 PSU and ocean temperatures are initialized with a depth dependent distribution (see Sepulchre et al., GMD 2020, in review). In waters deeper than 1000 m, the temperature, T=10°C, whereas at depths shallower than 1000 m it follows

$$T = 10 + \left(\frac{1000 - depth}{1000}\right) * 25\cos(latitude) \quad (1)$$

*Table 1 : Description of the simulations. The parameters in bold indicate the specific change for the corresponding simulation. Simulations are run for 2000 years, except piControl which is run for 1000 years.*

| Simulation | piControl | 1X-NOICE | 4X-NOICE | 4X-NOICE-PFT-SOIL | 4X-NOICE-PFT-SOIL-SOLAR | 4X-CRETACEOUS |
|---|---|---|---|---|---|---|
| Polar Caps | Yes | **No** | No | No | No | No |
| $CO_2$ (ppm) | 280 | 280 | **1120** | 1120 | 1120 | 1120 |
| Vegetation | IPCC (1850) | IPCC (1850) + Bare soil instead of polar caps | IPCC (1850) + Bare soil instead of polar caps | **Theoretical latitudinal PFTs** | Theoretical latitudinal PFTs | Theoretical latitudinal PFTs |
| Soil Color/Texture | IPCC (1850) | IPCC (1850) + Brown soil instead of polar caps | IPCC (1850) + Brown soil instead of polar caps | **Uniform mean value** | Uniform mean value | Uniform mean value |
| Solar constant ($W/m^2$) | 1365.6537 | 1365.6537 | 1365.6537 | 1365.6537 | **1353.36** | 1353.36 |
| Geographic configuration | Modern | Modern | Modern | Modern | Modern | **Cretaceous 90 Ma (Sewall 2007 + Müller 2008)** |

# 3. RESULTS

The simulated changes between the preindustrial (piControl) and the CT (4X-CRETACEOUS) simulations can be decomposed into five components based on our boundary condition changes: (1) Polar ice sheet removal (Δice), (2) $pCO_2$ ($\Delta CO_2$), (3) PFT and Soil parameters (ΔPFT-SOIL), (4) Solar constant (Δsolar) and (5) Paleogeography (Δpaleo). Each contribution to the total climate change can be calculated by a linear factorization (Broccoli and Manabe, 1987; Von Deimling et al., 2006), which simply corresponds to the anomaly between two consecutive simulations. The choice of applying a linear factorization approach was made due to computing time and cost. We appreciate that another sequence of changes could lead to different intermediate states and could modulate the intensity of warming or cooling associated to each change. The computational costs would be too high for this study to explore this further here; it is an interesting problem that we leave for a future investigation. The results presented in the following are averages calculated over the last 100 simulated years.

## 3.1 GLOBAL CHANGES

The progressive change of parameters made to reconstruct the CT climate induces a general global warming (Table 2, Fig. 3). The annual global atmospheric temperature at 2 meters above the surface (T2M) rises from 13.25°C to 24.35 °C between the preindustrial and CT simulations. All changes in boundary conditions generates a warming signal on a global scale, with the exception of the decrease in solar constant which generates a cooling. Most of the warming is due to the fourfold increase in atmospheric pCO2, which alone increases the global mean temperature by 9°C. Paleogeographic changes also represent a major contributor to the warming, leading to an increase in T2M of 2.6°C. In contrast, the decrease in solar constant leads to a cooling of 1.8°C at the global scale. Finally, changes in the soil parameters and PFTs, as well as the retreat of polar caps, have smaller impacts, leading to increases in global mean T2M of 0.8°C and 0.5°C respectively.

Temperature changes exhibit different geographic patterns (Fig. 4) depending on which parameter is changed. These patterns range from global and uniform cooling (Δsolar – Fig 4e) to a global, polar-amplified, warming ($\Delta pCO_2$ – Fig 4c), as well as heterogeneous regional responses (Δice or Δpaleo – Fig 4b and 4f). In the next section, we describe the main patterns of change and the main feedbacks arising.

| | piControl | 1X-NOICE | 4X-NOICE | 4X-NOICE-PFT-SOIL | 4X-NOICE-PFT-SOIL-SOLAR | 4X-CRETACEOUS |
|---|---|---|---|---|---|---|
| T2M (°C) | 13.25 | 13.75 | 22.75 | 23.55 | 21.75 | 24.35 |
| Planetary Albedo (%) | 33.1 | 32.6 | 28.8 | 28.3 | 28.7 | 27.1 |
| Surface Albedo (%) | 20.1 | 19 | 16.6 | 15.5 | 15.3 | 14.9 |
| Emissivity (%) | 62 | 61.7 | 57.5 | 57.1 | 57.8 | 57 |

*Table 2: Simulations results (Global annual mean over last 100 years of simulation.*

## 3.2 The major contributor to global warming - $\Delta CO_2$

As mentioned above, the fourfold increase in $pCO_2$ leads to a global warming of 9°C (Table 3, Fig. 3) between the 1X-NOICE and the 4X-NOICE simulations. The whole Earth warms, with an amplification located over the Arctic and Austral oceans and a warming generally larger over continents than over oceans (Fig 4c). The warming is due to a general decrease of planetary albedo and of the atmosphere's emissivity (see Supplementary Figure 2). The decrease in the atmosphere's emissivity is directly driven by the increase in $CO_2$, and thus greenhouse trapping in the atmosphere. It is also amplified by an increase in high-altitude cloudiness (defined as cloudiness at atmospheric pressure < 440 hPa) over the Antarctic continent (Fig 5a, b). The decrease in planetary albedo is due to two major processes. First, a decrease of sea ice and snow cover (especially over Northern Hemisphere continents and along the coasts of Antarctica), leading to surface albedo decrease, explains the warming amplification over polar oceans and continents. Second, a decrease in low-altitude cloudiness (defined as cloudiness at atmospheric pressure > 680 hPa) at all latitudes except over the Arctic (Fig 5a, b) leads to an increase in absorbed solar radiation.

The contrast in the atmospheric response over continents and oceans is due to the impact of the evapo-transpiration feedback. Oceanic warming drives an increase in evaporation, which acts as a negative feedback and moderates the warming by consuming more latent heat at the ocean surface. In contrast, high temperatures resulting from continental warming tend to inhibit vegetation development, which acts as positive feedback and enhances the warming due to reduced transpiration and reduced latent heat consumption.

## 3.3 Boundary conditions with the smallest global impact – $\Delta$ice, $\Delta$PFT-SOIL, $\Delta$solar

The removal of polar ice sheets in the 1X-NOICE simulation leads to a weak global warming of 0.5°C but a strong regional warming observed over areas previously covered by the Antarctic and Greenland ice sheets (Fig 4a, b). This signal is due to the combination of a decrease in elevation (i.e., lapse rate feedback – Supplementary Figure S3) and in surface albedo, which is directly linked to the

shift from a reflective ice surface to a darker bare soil surface. Unexpected cooling is also simulated in specific areas, such as the margins of the Arctic Ocean and the southwestern Pacific. These contrasted climatic responses to the impact of ice sheets on sea surface temperatures are consistent with previous modeling studies (Goldner et al., 2014; Knorr and Lohmann, 2014; Kennedy et al., 2015). Their origin is still unclear but changes in winds in the Southern Ocean, due to topographic changes after polar ice sheet removal, may locally impact oceanic currents, deep-water formation, and thus oceanic heat transport and temperature distribution. In the Northern Hemisphere, the observed cooling over Eurasia could be linked to stationary wave feedbacks following changes in topography after Greenland ice sheet removal (Supplementary Figure S4; see also Maffre et al., 2018).

The change in soil parameters and the implementation of theoretical zonal PFTs in the 4X-NOICE-PFT-SOIL simulation drive a warming of 0.8 °C. This warming is essentially located above arid areas, such as the Sahara, Australia, or Middle East, and polar latitudes (Antarctica/Greenland) (Fig 4d), and is mostly caused by the implementation of a mean uniform soil color, which drives a surface albedo decrease over deserts that normally have a lighter color. The warming at high-latitudes is linked to vegetation change: bare soil that characterizes continental regions previously covered with ice is replaced by boreal vegetation with a lower surface albedo. The presence of vegetation at such high-latitudes is consistent with high-latitude paleobotanical data and temperature records during the Cretaceous (Otto-bliesner and Upchurch, 1997; Herman and Spicer, 2010; Spicer and Herman, 2010).

Finally, the change in solar constant from 1365 W/m$^2$ to 1353 W/m$^2$ (Gough 1981) directly drives a cooling of 1.8 °C evenly distributed over the planet (Fig 4e).

### 3.4 The most complex response - Δpaleogeography

The paleogeographic change drives a global warming of 2.6 °C. This is seen year-round in the Southern Hemisphere, while the Northern Hemisphere experiences a warming during winter and cooling during summer compared to the 4X-NI-PFT-SOIL-SOLAR simulation (Fig 6). These temperature changes are linked to a general decrease in planetary albedo and/or emissivity, although the Northern Hemisphere sometimes exhibits increased albedo, due to the increase in low-altitude cloudiness. This increase in albedo is compensated by a strong atmosphere emissivity decrease during winter but not during summer, which leads to the seasonal pattern of cooling and warming (Supplementary Figure S5).

The albedo and emissivity changes are linked to atmospheric and oceanic circulation modifications driven by four major features of the CT paleogeography (Fig 2):

(1) Equatorial oceanic gateway opening (Central American Seaway/Neotethys)

(2) Polar gateway closure (Drake/Tasman)

(3) Increase in oceanic area in the North Hemisphere (Fig 2)

(4) Decrease in oceanic area in the South Hemisphere (Fig 2)

In the CT simulation, we observe an intensification of the meridional surface circulation and extension towards higher latitudes compared to the simulation with the modern geography (Fig8a-b), as well as an intensification of subtropical gyres, especially in the Pacific (Supplementary Figure S6), which are responsible for an increase in poleward oceanic heat transport (OHT – Fig 8c). Such modifications can be linked to the opening of equatorial gateways that creates a zonal connection between the Pacific, Atlantic and Neotethys oceans (Enderton and Marshall, 2008; Hotinski and Toggweiler, 2003) and that leads to the formation of a strong circumglobal equatorial current (Fig 7b) . This connection permits the existence of stronger easterly winds that enhance equatorial upwelling and drive increased export of water and heat from low latitudes to polar regions. In the Southern Hemisphere, the Drake Passage is only open to shallow flow, and the Tasman gateway has not yet formed. The closure of these zonal connections leads to the disappearance of the modern Antarctic Circumpolar Current (ACC) during the Cretaceous (Fig 7c-d). Notwithstanding, the observed increase in southward OHT between 40° and 60°S (Fig 8c) is explained by the absence of significant zonal connections in the Southern Ocean, which allows for the buildup of polar gyres in the CT simulation (Supplementary Figure S6).

The increase in OHT is associated with a meridional expansion of high sea-surface temperatures leading to an intensification of evaporation between the tropics and a poleward shift of the ascending branches of the Hadley cells. The combination of these two processes results in a greater injection of moisture into the atmosphere between the tropics (Supplementary Figure S7). Consequently, the high-altitude cloudiness increases and spreads towards the tropics, leading to an enhanced greenhouse effect. This process is the main driver of the intertropical warming (Herweijer et al., 2005; Levine and Schneider, 2010; Rose and Ferreira, 2013).

The atmosphere's response to the paleogeographic changes in the mid- and high-latitudes is different in the Southern and Northern Hemispheres because the ocean to land ratio varies between the CT configuration and the modern. In the Southern Hemisphere, the reduced ocean surface area in the CT simulation (Fig 2) limits evaporation and moisture injection into the atmosphere, which in turn leads to a decrease in relative humidity and low-altitude cloudiness (Supplementary Fig S8) and associated year-round warming due to reduced planetary albedo. In the Northern Hemisphere, oceanic surface area increases (Fig 2) and results in a strong increase in evaporation and moisture injection into the atmosphere. Low-altitude cloudiness and planetary albedo increase and lead to summer cooling, as discussed above (Fig 6). During winter an increase in high-altitude cloudiness leads to an enhanced greenhouse effect and counteracts the larger albedo. This high-altitude cloudiness

increase is consistent with the simulated increase in extratropical OHT (Fig. 8). Mid-latitude convection and moist air injection into the upper troposphere is consequently enhanced and efficiently transported poleward (Rose and Ferreira, 2013; Ladant and Donnadieu, 2016). In addition, increased continental fragmentation in the CT paleogeography relative to the preindustrial decreases the effect of continentality (Donnadieu et al. 2006) because thermal inertia is greater in the ocean than over continents.

## 3.5 Temperature Gradients

### 3.5.1 Ocean

The mean annual global SST increases as much as 9.8°C (from 17.9°C to 27.7 °C) across the simulations. The SST warming is slightly weaker than that of the mean annual global atmospheric temperature at 2m discussed above, and most likely occurs because of evaporation processes due to the weaker atmospheric warming simulated above oceans compared to that simulated above continents. Unsurprisingly, as for the atmospheric temperatures, $pCO_2$ is the major controlling parameter of the ocean warming (7°C), followed by paleogeography (4.5°C) and changes in the solar constant (2.3°C), although the latter induces a cooling rather than a warming. PFT and soil parameter changes and the removal of polar ice sheets have a minor impact at the global SST (0.6 °C and 0°C respectively). It is interesting to note the increased contribution of paleogeography to the simulated SST warming compared to its contribution to the simulated atmospheric warming, which is probably driven by the major changes simulated in surface ocean circulation (Fig. 7).

Mean annual SST in the preindustrial simulation reach ~ 26°C in the tropics (calculated as the zonal average between 30°S and 30°N) and ~ -1.5°C at the poles (beyond 70° N - Fig 9a). In this work, we define the meridional temperature gradients as the linear temperature change per 1° of latitude between 30° and 80°. The gradients in the piControl experiment then amount to 0.45°C/°latitude and 0.44°C/°latitude for the Northern and Southern Hemispheres, respectively. In the CT simulation, the mean annual SST reach ~ 33.3°C in the tropics, and ~5°C and 10°C in the Arctic and Southern Ocean respectively, and the simulated CT meridional gradients are 0.45°C/°latitude and 0.39°C/°latitude for the Northern and Southern Hemispheres, respectively.

The progressive flattening of the SST gradient can be visualized by superimposing the zonal mean temperatures of the different simulations and by adjusting them at the Equator (Fig 9b). Two major observations can be drawn from these results. First, paleogeography has a strong impact on the low-latitudes (< 30° of latitude) SST gradient because it widens the latitudinal band of relatively homogeneous warm tropical SST as a result of the opening of equatorial gateways. Second, poleward of 40° in latitude, the paleogeography and the increase in atmospheric $pCO_2$ both contribute to the

flattening of the SST gradient with a larger influence from paleogeography than from atmospheric $pCO_2$.

### 3.5.2 Atmosphere

In the preindustrial simulation, mean tropical atmospheric temperatures reach ~ 23.6°C whereas polar temperatures (calculated as the average between 80° and 90° of latitude) in the Northern and Southern Hemispheres reach around -16.8°C and -37°C respectively. The northern meridional temperature gradient is 0.69°C/°latitude while the southern latitudinal temperature gradient is 1.07°C/°latitude (Fig 9c). This significant difference is explained by the very negative mean annual temperatures over Antarctica linked to the presence of the ice sheet.

In the CT simulation, mean tropical atmospheric temperatures reach ~ 32.3°C whereas polar temperatures reach ~ 3.4°C in the Northern Hemisphere and ~ - 0.5°C in the Southern Hemisphere, thereby yielding latitudinal temperature gradients of 0.49°C/°latitude and 0.54°C/°latitude, respectively. The gradients are reduced compared to the preindustrial because the absence of year-round sea and land ice at the poles drives leads to far higher polar temperatures.

As for the SST gradients, we plot atmospheric meridional gradients by adjusting temperature values so that temperatures at the Equator are equal for each simulation (Fig 9d). This normalization reveals that the mechanisms responsible for the flattening of the gradients are different for each hemisphere. In the Southern Hemisphere high-latitudes (> 60° of latitude), three parameters contribute to reducing the equator-to-pole temperature gradient in the following order of importance: removal of polar ice sheets, paleogeography and increase in atmospheric $pCO_2$. In contrast, the reduction in the gradient steepness in the Northern Hemisphere high-latitudes is exclusively explained by the increase in atmospheric $pCO_2$. In the low- and mid-latitudes, this temperature gradient reduction is essentially explained by paleogeography in the Southern Hemisphere and by a similar contribution of paleogeographic changes and increase in atmospheric $pCO_2$ in the Northern Hemisphere.

## 4. DISCUSSION

### 4.1 CENOMANIAN-TURONIAN MODEL/DATA COMPARISON

The results predicted by our CT simulation can be compared to reconstructions of atmospheric and oceanic paleotemperatures inferred from proxy data (Fig 10a, b). Our SST data compilation is modified version of Tabor et al (2016), with additional data from more recent studies (see our Supplementary data). We also compiled atmospheric temperature data obtained from

paleobotanical and paleosoil studies (see Supplementary data for the complete database and references).

The Cretaceous equatorial and tropical SST have long been believed to be similar or even lower than those of today (Sellwood et al., 1994; Crowley and Zachos, 1999; Huber et al., 2002), thus feeding the problem of "tropical overheating" systematically observed in General Circulation Model simulations (Barron et al., 1995; Bush et al., 1997; Poulsen et al., 1998). This incongruence was based on the relatively low tropical temperatures reconstructed from foraminiferal calcite (25-30°C, Fig. 9a), but subsequent work suggested that these were underestimated because of diagenetic alteration (Pearson et al., 2001; Pucéat et al., 2007). Latest data compilations including temperature reconstructions from other proxies, such as TEX86, have provided support for high tropical SST in the Cenomanian-Turonian (Tabor et al., 2016; O'Brien et al., 2017) and our tropical SST are mostly consistent with existing paleotemperature reconstructions (Fig. 10a). In the mid-latitudes (30-60°), proxy records infer a wide range of possible SST, ranging from 10°C to more than 30°C. Simulated temperatures in our CT simulation reasonably agree with these reconstructions if seasonal variability, represented by local monthly maximum and minimum temperatures (grey shaded areas, Fig 10a), is considered. This congruence would imply that a seasonal bias may exist in temperatures reconstructed from proxies, which is suggested in previous studies (Sluijs et al., 2006; Hollis et al., 2012; Huber, 2012; Steinig et al., 2020) but still debated (Tierney, 2012). There are unfortunately only a few high-latitudes SST data points available, which render the model-data comparison difficult. In the Northern Hemisphere, the presence of crocodilian fossils (Vandermark et al., 2007) in the northern Labrador Sea (~70° of latitude) imply mean annual temperature of at least 14°C and temperature of the coldest month of at least 5°C. In comparison, simulated temperatures at the same latitude in the adjacent Western Interior Sea are very similar (13.5 °C for the annual mean and 7.9 °C for the coldest month). In the Southern Hemisphere, mean annual SST calculated from foraminiferal calcite at DSDP sites 511 and 258 are between 25° and 28°C (Huber et al., 2018). Simulated annual SST reach a monthly maximum of 28°C around the location of site DSDP 258. We speculate that a seasonal bias in the foraminiferal record may represent a possible cause for this difference; alternatively, local deviations of the regional seawater $\delta^{18}O$ from the globally assumed -1‰ value may also reduce the model-data discrepancy (Zhou et al., 2008; Zhu et al., 2020).

To our knowledge, atmospheric temperature reconstructions from tropical latitudes are not available. In the mid-latitudes (30-60°), simulated atmospheric temperatures in the Southern Hemisphere reveal reasonable agreement with data whereas Northern Hemisphere mean zonal temperatures in our model are slightly warmer than that inferred from proxies (Fig 10b). At high-latitudes, the same trend is observed for atmospheric temperatures as it is for SST with data indicating higher temperatures than the model in both the Southern and Northern Hemispheres. This inter-

hemispheric symmetry in model-data discrepancy could indicate a systematic cool bias of the simulated temperatures.

### 4.2 RECONSTRUCTED LATITUDINAL TEMPERATURE GRADIENTS

The simulated northern hemisphere latitudinal SST gradient of (~0.45°C/°latitude) is in good agreement with those reconstructed from paleoceanographic data in the Northern Hemisphere (~0.42°C/°latitude) whereas it is much larger in the Southern Hemisphere (~0.39°C/°latitude vs ~0.3°C/°latitude) (Fig 11). This overestimate of the latitudinal gradient holds for the atmosphere as well, as gradients inferred from data are much lower (North=0.2°C/°latitude and South=0.18°C/°latitude) than simulated gradients (North=0.49°C/°latitude and South=0.55°C/°latitude), although the paucity of Cenomanian-Turonian continental temperatures proxy data is likely to significantly bias this comparison.

In the following, we compare our simulated gradients to those obtained in previous deep time modelling studies using recent earth system models. Because Earth system models studies focusing on the Cenomanian-Turonian are limited in numbers, we include simulations of the Early Eocene (~ 55 Ma), which is another interval of global climatic warmth (Lunt et al., 2012a, 2017) (Fig. 11). The simulated SST latitudinal gradients range from 0.32°C/°latitude to 0.55°C/°latitude (Lunt et al., 2012; Tabor et al., 2016; Zhu et al., 2019; Fig. 11) and the atmospheric latitudinal gradients from 0.33°C/°latitude to 0.78°C/°latitude (Huber and Caballero, 2011; Lunt et al., 2012; Niezgodzki et al., 2017; Upchurch et al., 2015; Zhu et al., 2019; Fig. 11). For a single model and a single set of boundary conditions (Cretaceous or Eocene), the lowest latitudinal gradient is obtained for the highest $pCO_2$ value. However, when comparing different studies with the same model (Cretaceous vs Eocene using the ECHAM5 model; Lunt et al., 2012a; Niezgodzki et al., 2017) it is not the case: the South Hemisphere atmospheric gradient obtained for the Eocene with the ECHAM5 model is always lower than those obtained for the Cretaceous with the same model, regardless of the $pCO_2$ value (Fig. 11 and Supplementary Data). These results show the major role of boundary conditions (in particular paleogeography) in defining the latitudinal temperature gradient. IPSL-CM5A2 predicts SST and atmosphere gradients that are well within the range of other models of comparable resolution and complexity. Models almost systematically simulate larger gradients than those obtained from data (Fig. 11, see also Huber, 2012). The reasons behind this incongruence are debated (Huber, 2012) but highlight the need for more data and for challenging the behavior of complex earth system models, in particular in the high latitudes. Studies have demonstrated that models are able to simulate lower latitudinal temperature gradients under specific conditions such as anomalously high $CO_2$ concentrations (Huber and Caballero, 2011), modified cloud properties and radiative parameterizations (Upchurch et al., 2015; Zhu et al., 2019) or lower paleo elevations and/or more

extensive wetlands (Hay et al., 2019). Finally, from a proxy perspective, it has been suggested that a sampling bias could exist, with a better record of temperatures during the warm season at high latitudes and during the cold season in low latitudes (Huber, 2012). Such possible biases would help reduce the model-data discrepancy, in particular for atmospheric temperatures (Fig 10b), as high-latitude reconstructed temperatures are more consistent with simulated summer temperatures whereas the consistency is better with simulated winter temperatures in the mid- to low-latitudes, but further work is required to unambiguously demonstrate the existence of these biases.

## 4.3 PRIMARY CLIMATE CONTROLS

The earliest estimates of climate sensitivity (or the temperature change under a doubling of the atmospheric $pCO_2$) predicted a 1.5 to 4.5°C temperature increase, with the most likely scenario providing an increase of 2.5°C (Charney et al., 1979; Barron et al., 1995; Sellers et al., 1996; IPCC, 2014). Our modelling study predicts an atmospheric warming of 11.1°C for the CT. The signal is notably due to a 9°C warming in response to the fourfold increase in $pCO_2$, which converts to an increase of 4.5°C for a doubling of $pCO_2$ (assuming a linear response). This climate sensitivity agrees with the higher end of the range of previous estimates (Charney et al., 1979; Barron et al., 1995; Sellers et al., 1996; IPCC, 2014). However, our simulated climate sensitivity could be slightly lower as the simulations are not completely equilibrated (Fig. 1). The latest generation of Earth system models used in deep-time paleoclimate also show an increasingly higher climate sensitivity to increased $CO_2$ (Hutchinson et al., 2018; Golaz et al., 2019; Zhu et al., 2019), suggesting that the sensitivity could have been underestimated in earlier studies. For example, the recent study of Zhu (2019), using an up-to-date parameterization of cloud microphysics in the CESM1.2 model, proposes an Eocene Climate Sensitivity of 6.6°C for a doubling of $CO_2$ from 3 to 6 PAL.

We have shown that $pCO_2$ is the main controlling factor for atmospheric global warming whereas the effects of the paleogeography (warming) and reduced solar constant (cooling) nearly cancel each other out at the global scale (see also Lunt et al., 2016). These results agree with previous studies suggesting that $pCO_2$ is the main factor controlling climate (Barron et al., 1995; Crowley and Berner, 2001; Royer et al., 2007; Foster et al., 2017). However, we also demonstrate that paleogeography plays a major role in the latitudinal distribution of temperatures and impacts oceanic temperatures (with a similar magnitude than a doubling of $pCO_2$), thus confirming that it is also a critical driver of the Earth's climate (Poulsen et al., 2003; Donnadieu et al., 2006; Fluteau et al., 2007; Lunt et al., 2016). The large climatic influence of the continental configuration has not been reported for paleogeographic configurations closer to each other, e.g., the Maastrichtian and Cenomanian (Tabor et al., 2016). The main features influencing climate in our study (i.e. the configuration of

equatorial and polar zonal connections and the land/sea distribution) are indeed not fundamentally different in the two geological periods investigated by Tabor et al. (2016). Paleogeography is thus a first-order control on climate over long timescales.

Early work has suggested that high latitude warming can be amplified in deep time simulations by rising $CO_2$ via cloud and vegetation feedbacks (Otto-bliesner and Upchurch, 1997; Deconto et al., 2000) or by increasing ocean heat transport (Barron et al., 1995; Schmidt and Mysak, 1996; Brady et al., 1998), in particular when changing the paleogeography (Hotinski and Toggweiler, 2003). Our study confirms that the paleogeography is a primary control on the steepness of the oceanic meridional temperature gradient. Furthermore, paleogeography is the only process, among those investigated, that controls both the atmosphere and ocean temperature gradients in the tropics and it has a greater impact than atmospheric $CO_2$ on the reduction of the atmospheric temperature gradient at high latitudes in the Southern Hemisphere between the CT and the preindustrial. The increase in $pCO_2$ appears as the second most important parameter controlling the SST gradient at high latitudes and is the main control of the reduced atmospheric gradient in the Northern Hemisphere due to low cloud albedo feedback. The effect of paleovegetation on the reduced temperature gradient is marginal at high latitudes in our simulations, in contrast to the significant warming reported in early studies (Otto-bliesner and Upchurch, 1997; Upchurch, 1998; Deconto et al., 2000) but in agreement with more recent model simulations suggesting a limited influence of vegetation in the Cretaceous high-latitudes warmth (Zhou et al., 2012). However, our modeling setup prescribes boreal vegetation at latitudes higher than 50° whereas evidence exist to support the development of evergreen forests poleward of 60° of latitude (Sewall et al., 2007; Hay et al., 2019) and of temperate forests up to 60° of latitude (Otto-bliesner and Upchurch, 1997). The presence of such vegetation types could change the albedo of continental regions but also heat and water vapor transfer by altered evapo-transpiration processes, thus leading to warming amplification at high-latitudes and reduced temperature gradients (Otto-bliesner and Upchurch, 1997; Hay et al., 2019). Based on these studies and on our results, we cannot exclude that different types of high-latitude could promote a greater impact of paleovegetation in reducing the temperature gradient.

## 5. CONCLUSIONS

To quantify the impact of major climate forcings on the Cenomanian-Turonian climate, we perform a series of 6 simulations using the IPSL-CM5A2 earth system model in which we incrementally implement changes in boundary conditions on a preindustrial simulation to obtain ultimately a simulation of the Cenomanian-Turonian stage of the Cretaceous. This study confirms the primary control exerted by atmospheric $pCO_2$ on atmospheric and sea-surface temperatures, followed by

paleogeography. In contrast, the flattening of meridional SST gradients between the preindustrial and the CT is mainly due to paleogeographic changes and to a lesser extent to the increase in $pCO_2$. The atmospheric gradient response is more complex because the flattening is controlled by several factors including paleogeography, pCO2 and polar ice sheet retreat. While predicted oceanic and atmospheric temperatures show reasonable agreement with data in the low and mid latitudes, predicted temperatures in the high latitudes are colder than paleotemperatures reconstructed from proxies, which leads to steeper equator-to-pole gradients in the model than those inferred from proxies. However, this mismatch, often observed in data-model comparison studies, has been reduced in the last decades and could be further resolved by considering possible sampling/seasonal biases in the proxies and by continuously improving model physics and parameterizations.

# DATA AVAILABILITY

Code availability:

LMDZ, XIOS, NEMO and ORCHIDEE are released under the terms of the CeCILL license. OASIS-MCT is released under the terms of the Lesser GNU General Public License (LGPL). IPSL-CM5A2 code is publicly available through svn, with the following command lines: svn co http://forge.ipsl.jussieu.fr/igcmg/svn/modipsl/branches/publications/IPSLCM5A2.1_11192019 modipsl

cd modipsl/util;./model IPSLCM5A2.1

The mod.def file provides information regarding the different revisions used, namely:

– NEMOGCM branch nemo_v3_6_STABLE revision 6665

– XIOS2 branchs/xios-2.5 revision 1763

– IOIPSL/src svn tags/v2_2_2

– LMDZ5 branches/IPSLCM5A2.1 rev 3591

– branches/publications/ORCHIDEE_IPSLCM5A2.1.r5307 rev 6336

– OASIS3-MCT 2.0_branch (rev 4775 IPSL server)

The login/password combination requested at first use to download the ORCHIDEE component is anonymous/anonymous. We recommend to refer to the project website: http://forge.ipsl.jussieu.fr/igcmg_doc/wiki/Doc/Config/IPSLCM5A2 for a proper installation and compilation of the environment.

Data availability: Data that support the results of this study, as well as boundary condition files are available on request to the authors.

# AUTHOR CONTRIBUTION

M.L performed and analyzed the numerical simulations, in close cooperation with Y.D and J.B.L, and led the writing. M.G run the OTIS model to provide the Cenonamian-Turonian tidal dissipation. All authors discussed the results and analyses presented in the final version of the manuscript.

# COMPETING INTERESTS

The authors declare that they do not have competing interests.

# AKNOWLEDGMENTS

We express our thanks to Total E&P for funding the project and granting permission to publish. We thank the CEA/CCRT for providing access to the HPC resources of TGCC under the allocation 2018-GEN2212 made by GENCI. J.A.M.G receives funding from the Natural Environmental Research Council (grant NE/S009566/1, MATCH). We acknowledge use of the Ferret (ferret.pmel.noaa.gov/Ferret/) program for analysis and graphics in this paper.

# FIGURES

*Figure 1: Time series for mean annual oceanic temperatures. (a) Sea-surface temperature and (b) deep-ocean (2500 m) temperature. The piControl and 1X-NOICE simulations are perfectly equilibrated. The 4X simulations still have a small linear drift, around 0.1°C/century or less : 0.07, 0.08, 0.05 and 0.01°C/century during the last 500 years for SST of 4X-NOICE, 4X-NOICE-PFT-SOIL, 4X-NOICE-PFT-SOIL-SOLAR and 4X-CRETACEOUS respectively; 0.11, 0.08, 0.07 and 0.06°C/century during the last 500 years, for deep-ocean of 4X-NOICE, 4X-NOICE-PFT-SOIL, 4X-NOICE-PFT-SOIL-SOLAR and 4X-CRETACEOUS respectively.*

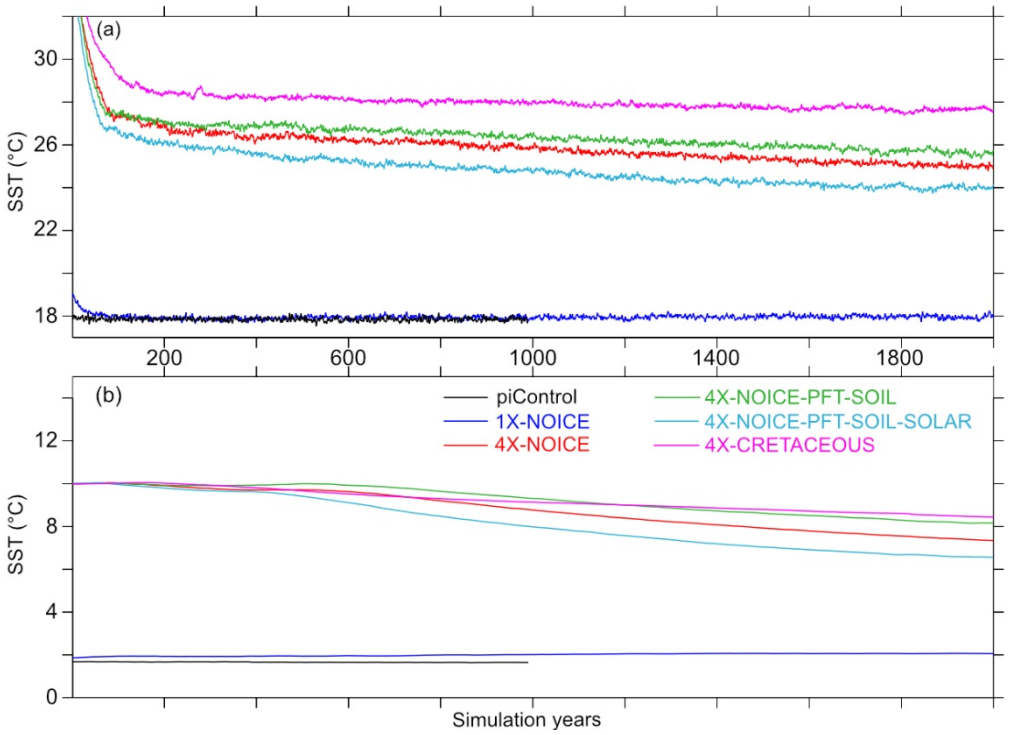

*Figure 2: Modern and Cenomanian-Turonian geographic configurations used for the piControl and 4X-CRETACEOUS simulations respectively, and meridional oceanic area anomaly between Cretaceous paleogeography and Modern. geography.*

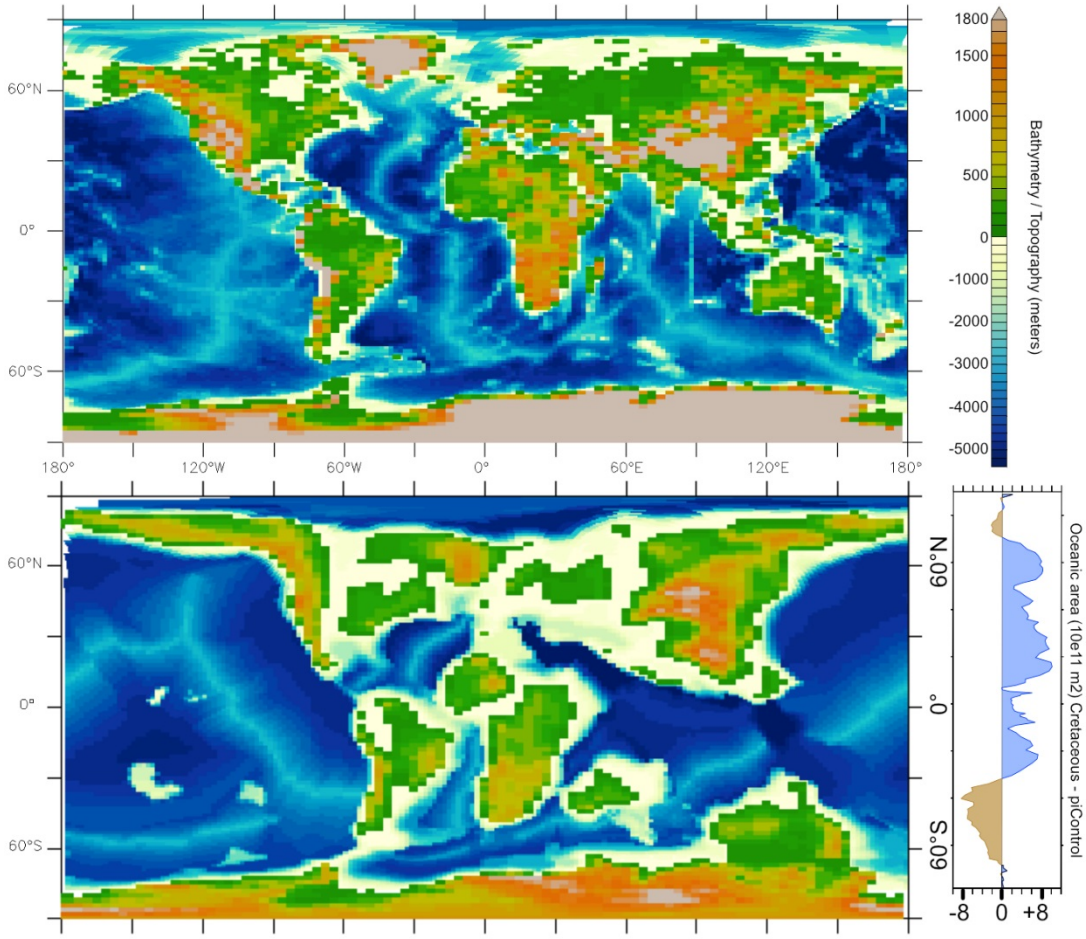


*Figure 3: Evolution of Albedo (surface and planetary) and emissivity, in percentages and of T2M (°C) from piControl to 4X-CRETACEOUS simulations. The major change is always recorded with the change of $pCO_2$ between 1X-NOICE and 4X-NOICE simulations.*

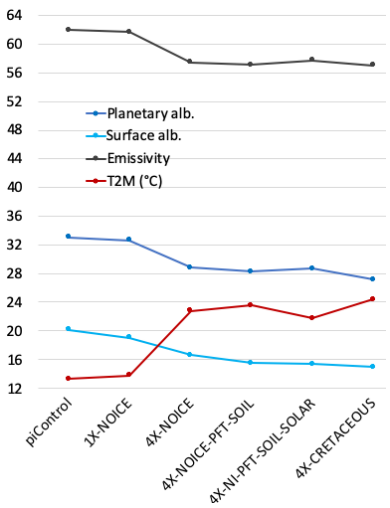

*Figure 4: T2M (°C) for (a) piControl initial simulation and (g) Cretaceous final simulation, and anomalies (°C) for intermediate simulations: (b) 1X-NOICE-piControl, (c) 4X-NOICE-1X-NOICE, (d) 4X-NOICE-PFT-SOIL – 4X-NOICE, (e) 4X-NOICE-PFT-SOIL-SOLAR – 4X-NOICE-PFT-SOIL, (f) 4X-CRETACEOUS - 4X-NOICE-PFT-SOIL. White color (not represented in the colourbar) correspond to areas where the anomaly is not statistically significative according to the student test.*

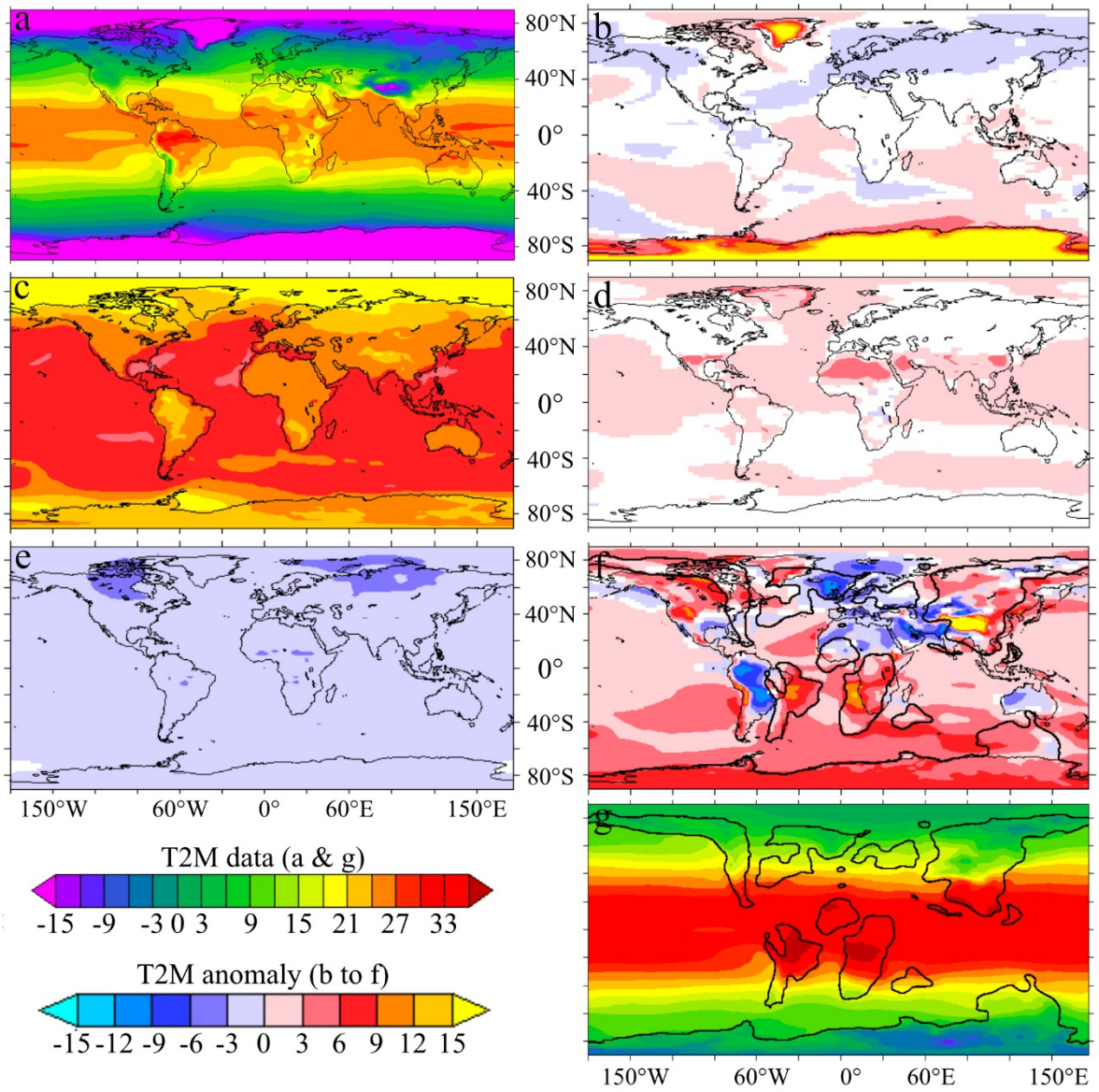

*Figure 5: Mean annual cloudiness for 1X-NOICE and 4X-NOICE simulations. (a) Anomaly of total cloudiness (4X-NOICE – 1X NOICE). (b) Low-altitude cloudiness (Below 680 hPa of atmospheric pressure - solid curves) and high-altitude cloudiness Above 440 hPa of atmospheric pressure - dashed curves) for 1X-NOICE (black) and 4X-NOICE (red) simulations.*

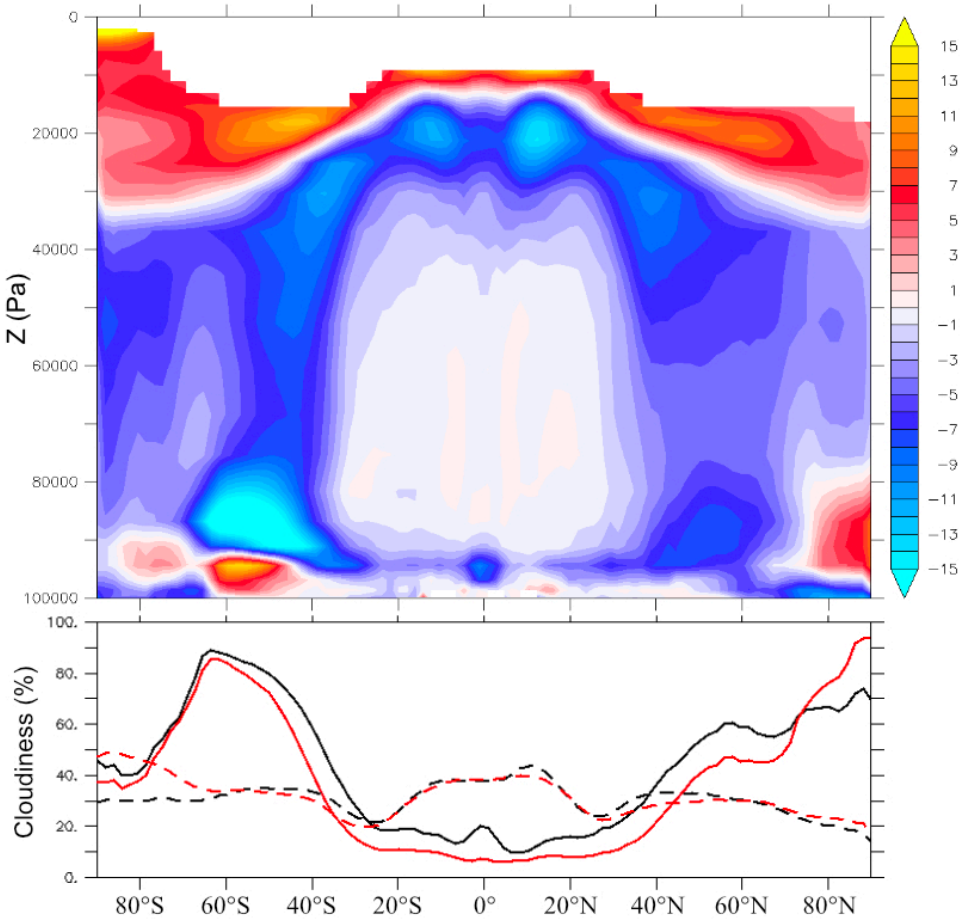


*Figure 6: T2M (°C) mean annual meridional gradients for 4X-NI-PFT-SOIL-SOLAR (black) and 4X-CRETACEOUS (red) simulations. Solid curve corresponds to annual average, dashed curves correspond to winter and summer values. The 4X-CRETACEOUS simulation is generally warmer than the 4X-NI-PFT-SOIL-SOLAR-SOLAR simulation, with the exception of the boreal summer.*

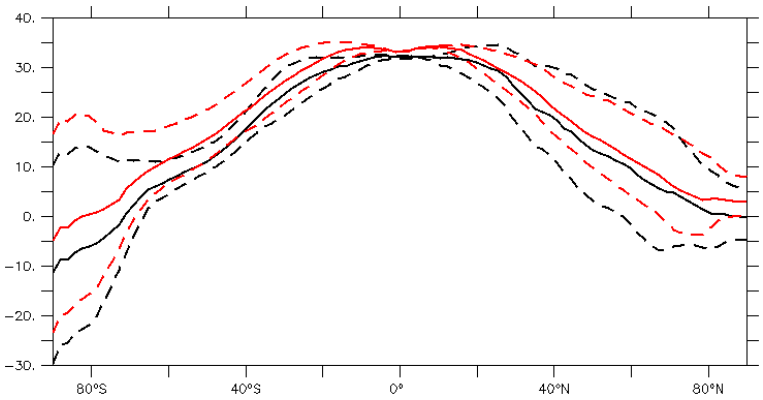

*Figure 7: Surface currents for 4X-NOICE-PFT-SOIL-SOLAR (left) and 4X-CRETACEOUS (right) simulations. (a), (b) Intensity of surface circulation (Sv – Annual Mean for 0-80 meters of water depth). Strong equatorial winds lead to the formation of an equatorial circumglobal current. (c), (d) Intensity of surface circulation (Sv – Annual Mean for 0-80 meters of water depth). The closure of the Drake passage (DP-300 meters of water depth) leads to the suppression of the ACC.*

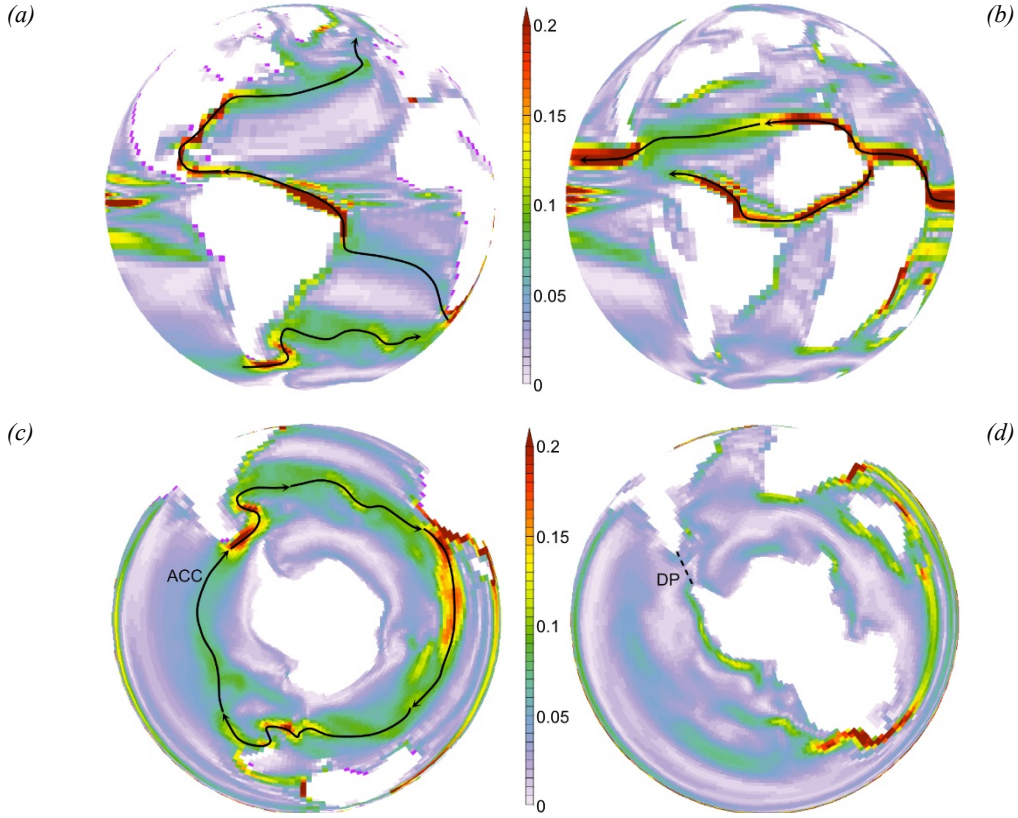

*Figure 8 - (a), (b) Global mean annual meridional stream-function (Sv) for the first 300 meters of water depth. Red and blue colors indicate clockwise and anti-clockwise circulation respectively. (a): 4X-NI-PFT-SOIL-SOLAR and (b) 4X-CRETACEOUS. (c) Oceanic heat transport for 4X-NI-PFT-SOIL-SOLAR and 4X-CRETACEOUS simulations. Positive and negative values indicate northward and southward transport direction, respectively.*

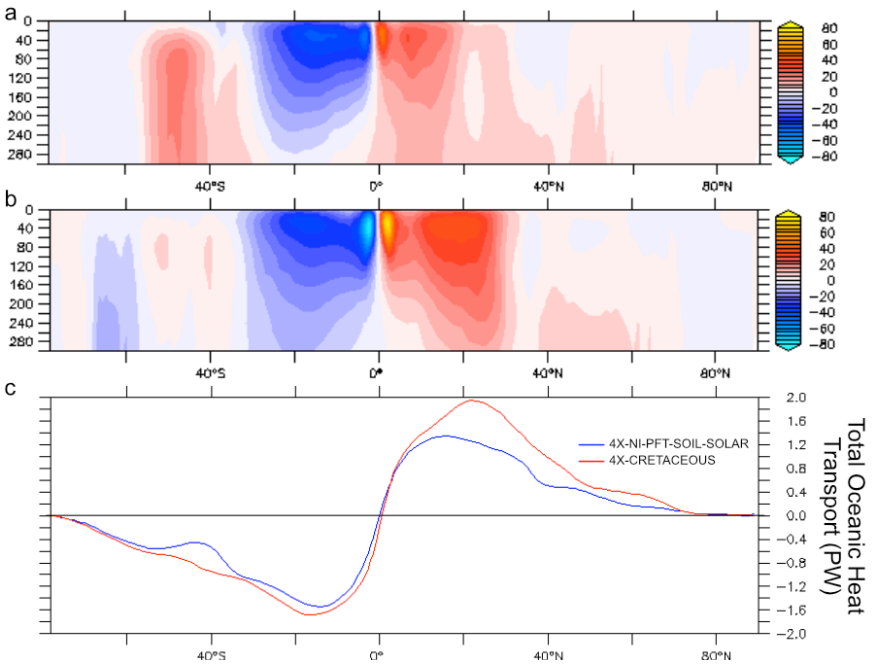


*Figure 9: (a) Mean annual meridional Sea-Surface Temperature gradients for all simulations. (b) Same SST curves than (a) but superimposed such as equator temperatures are equal, allowing to compare the steepness of the curves. (c) Meridional atmospheric surface temperature gradients for all simulations. (d) Same curves than (c) but superimposed such as equator temperatures are equal.*

*(a)* *(b)*

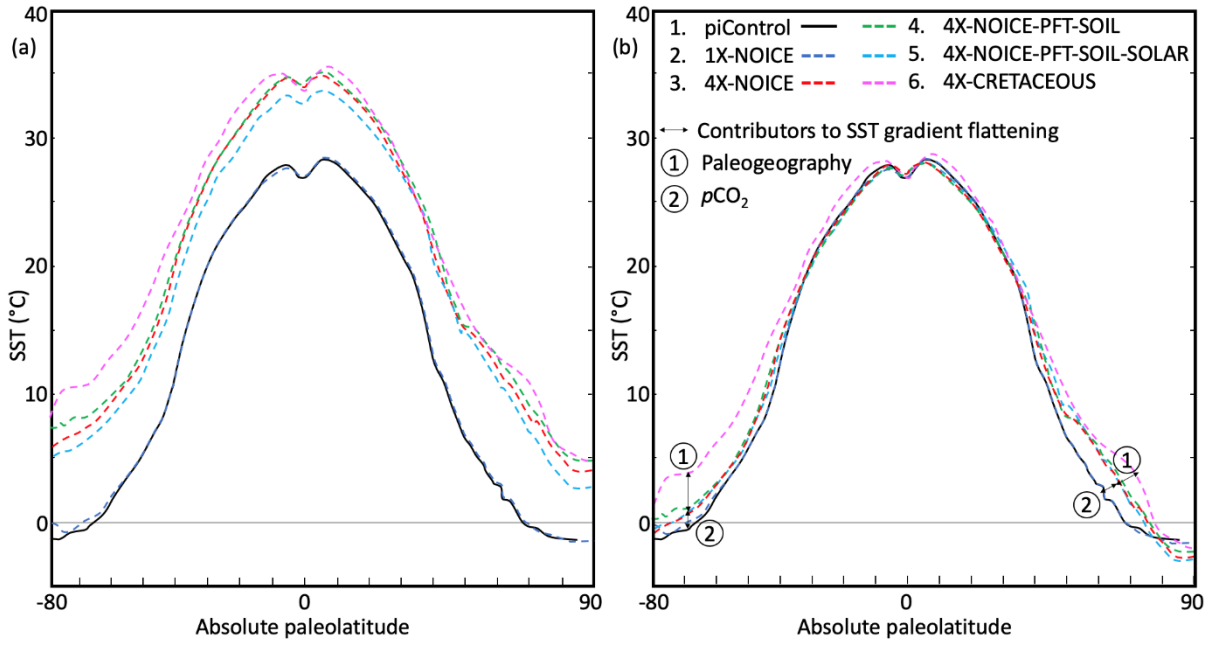


*(c)* *(d)*

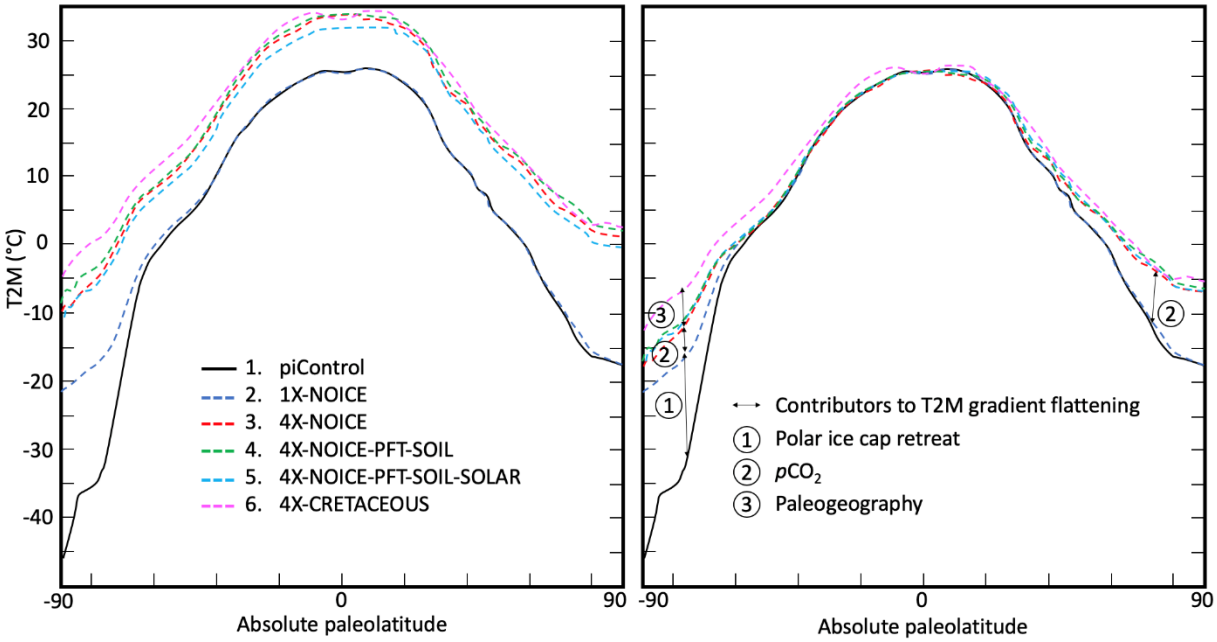


*Figure 10: Meridional surface temperature gradients for the 4X-CRETACEOUS simulation. (a) Oceanic temperatures: the solid line corresponds to the mean annual temperature obtained from the modeling. Dashed lines correspond to winter and summer seasonal averages. The grey shaded areas correspond to local monthly temperatures. Data points are obtained with several proxies for the Cenomano-Turonian period. The green data point is obtained from TEX 86 for the Maastrichtian (70 Ma) and extrapolated for 90 Ma. The Huber et al. (2018) point is obtained from $\delta^{18}0$ on foraminifera and the Vandenmark et al., 2007 point is interpreted from the presence of crocodilian fossils. MAT=Mean Annual Temperature, CM=Coldest Month. (b) Atmospheric temperatures: same legend as (a) for modelized temperatures. Data points are obtained from several proxies including CLAMP analysis on paleofloras, leaf analyses, paleosol-derived climofunction or bioclimatic analysis. Symbols represent mean annual temperatures and solid lines associated ranges/errors. Dashed lines represent monthly mean temperatures. Orange data points are for Cenomano-Turonian ages (100-90 Ma), blue data points for Albian and green data points for Coniacian-Santonian (88-85 Ma).*

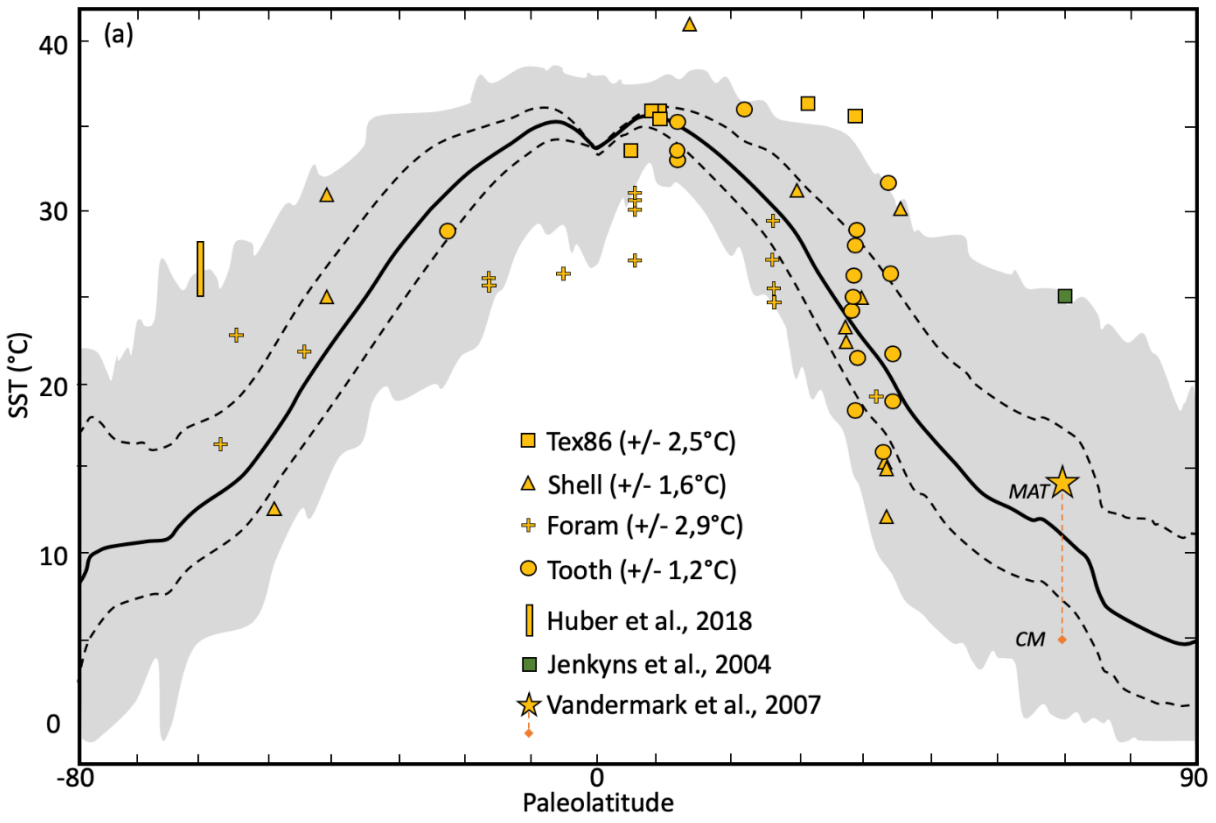
(a)
SST (°C)
40
30
20
10
0
-80
0
90
Paleolatitude
Tex86 (+/- 2,5°C)
Shell (+/- 1,6°C)
Foram (+/- 2,9°C)
Tooth (+/- 1,2°C)
Huber et al., 2018
Jenkyns et al., 2004
Vandermark et al., 2007
MAT
CM

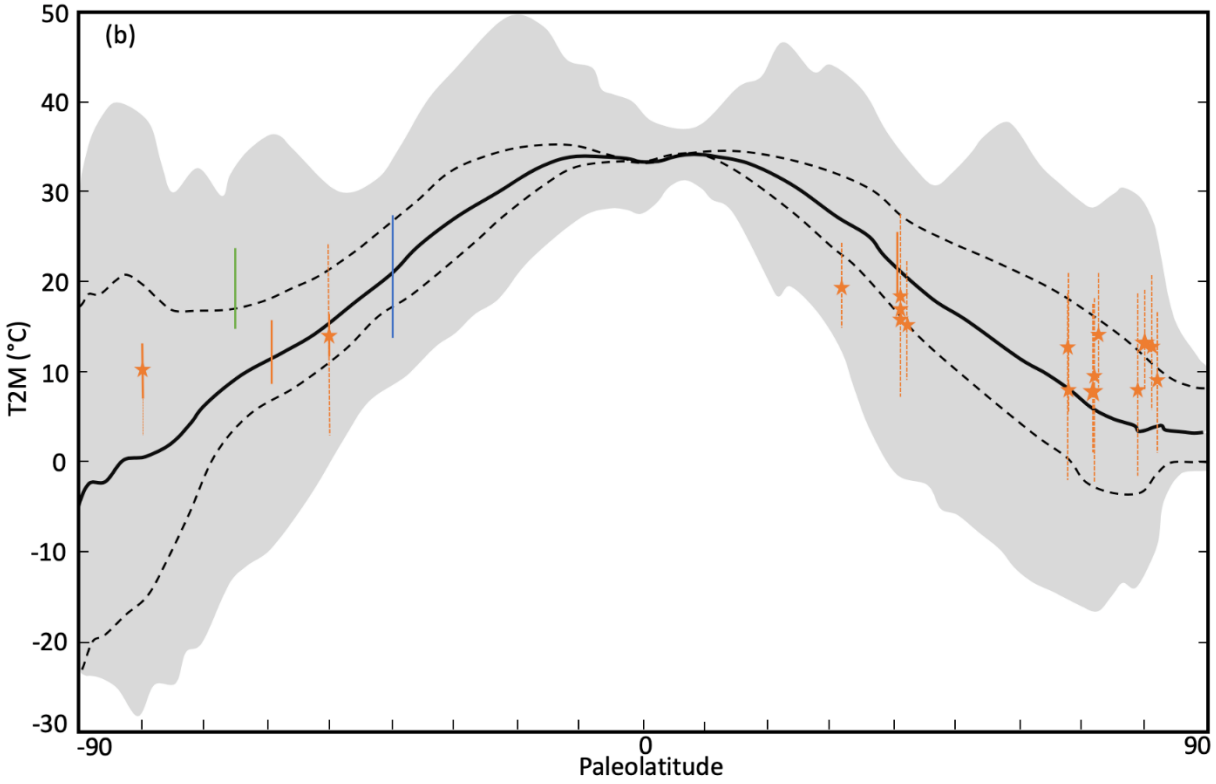
(b)
T2M (°C)
50
40
30
20
10
0
-10
-20
-30
-90
0
90
Paleolatitude

*Figure 11: Plot of atmospheric and sea surface mean annual temperature gradients vs $pCO_2$ for different modelling studies and data compilation. Data gradients are plotted for a default $pCO_2$ value of 4 P.A.L. Gradients are expressed in °C per °latitude and are calculated from 30 to 80 degrees of latitude. Gradients linked by a line correspond to studies realized with the same model & paleogeography. Solid lines or gradients marked with a (E) correspond to an Eocene paleogeography. Dashed lines or gradients marked with a C correspond to a Cretaceous paleogeography.*

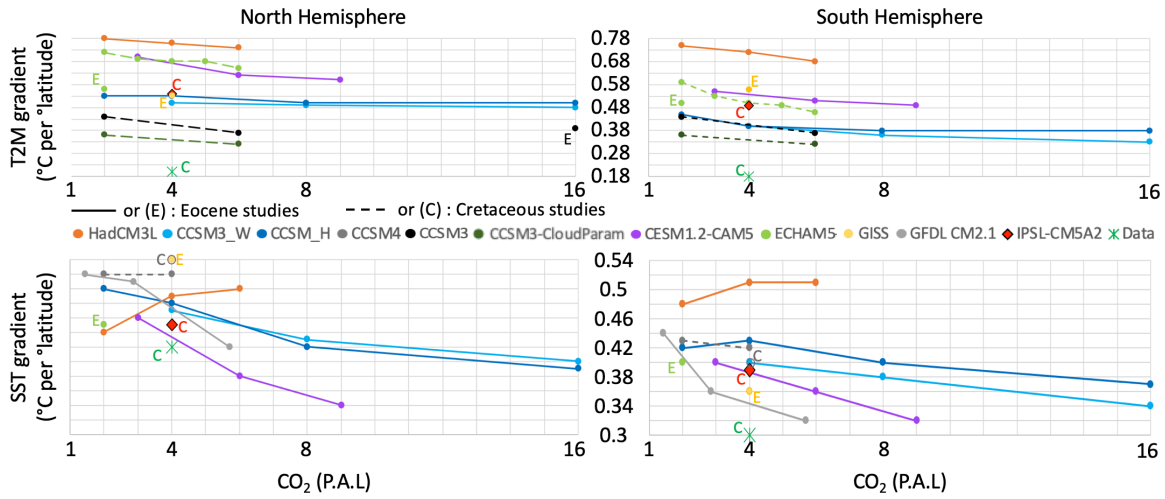


# REFERENCES


Aumont, O. and Bopp, L.: Globalizing results from ocean in situ iron fertilization studies, Global Biogeochem. Cycles, 20(2), 1–15, doi:10.1029/2005GB002591, 2006.

Aumont, O., Ethé, C., Tagliabue, A., Bopp, L. and Gehlen, M.: PISCES-v2: An ocean biogeochemical model for carbon and ecosystem studies, Geosci. Model Dev., 8(8), 2465–2513, doi:10.5194/gmd-8-2465-2015, 2015.

Barclay, R. S., McElwain, J. C. and Sageman, B. B.: Carbon sequestration activated by a volcanic CO 2 pulse during Ocean Anoxic Event 2, Nat. Geosci., 3(3), 205–208, doi:10.1038/ngeo757, 2010.

Barron, E. J.: Model simulations of Cretaceous climates : the role of geography and carbon dioxide, , 1(1989), 1993.

Barron, E. J., Fawcett, P. J., Peterson, W. H., Pollard, D. and Thompson, S. L.: A " simulation " of mid-Cretaceous climate Abstract . A series of general circulation model experiments W increased from present day ). By combining all three major variables levels of CO2 . Four times present-day • s W provided the best match to the this, , 10(5), 953–962, 1995.

Van Bentum, E. C., Reichart, G. J., Forster, A. and Sinninghe Damsté, J. S.: Latitudinal differences in the amplitude of the OAE-2 carbon isotopic excursion: PCO2and paleo

1472 productivity, Biogeosciences, 9(2), 717–731, doi:10.5194/bg-9-717-2012, 2012.
1473 Berner, R. A.: GEOCARBSULF: A combined model for Phanerozoic atmospheric O2 and
1474 CO2, Geochim. Cosmochim. Acta, 70(23 SPEC. ISS.), 5653–5664,
1475 doi:10.1016/j.gca.2005.11.032, 2006.
1476 Bice, K. L. and Norris, R. D.: Possible atmospheric CO 2 extremes of the Middle Cretaceous
1477 (late Albian-Turonian) , Paleoceanography, 17(4), 22-1-22–17, doi:10.1029/2002pa000778,
1478 2003.
1479 Bice, K. L., Birgel, D., Meyers, P. A., Dahl, K. A., Hinrichs, K. U. and Norris, R. D.: A
1480 multiple proxy and model study of Cretaceous upper ocean temperatures and atmospheric
1481 CO2 concentrations, Paleoceanography, 21(2), 1–17, doi:10.1029/2005PA001203, 2006.
1482 Bopp, L., Resplandy, L., Orr, J. C., Doney, S. C., Dunne, J. P., Gehlen, M., Halloran, P.,
1483 Heinze, C., Ilyina, T., Séférian, R., Tjiputra, J. and Vichi, M.: Multiple stressors of ocean
1484 ecosystems in the 21st century: Projections with CMIP5 models, Biogeosciences, 10(10),
1485 6225–6245, doi:10.5194/bg-10-6225-2013, 2013.
1486 Bopp, L., Resplandy, L., Untersee, A., Le Mezo, P. and Kageyama, M.: Ocean
1487 (de)oxygenation from the Last Glacial Maximum to the twenty-first century: Insights from
1488 Earth System models, Philos. Trans. R. Soc. A Math. Phys. Eng. Sci., 375(2102),
1489 doi:10.1098/rsta.2016.0323, 2017.
1490 Brady, E. C., Deconto, R. M. and Thompson, S. L.: Deep Water Formation and Poleward
1491 Ocean Heat Transport in the Warm Climate Extreme of the Cretaceous ( 80 Ma ) evidence, ,
1492 25(22), 4205–4208, 1998.
1493 Broccoli, A. J. and Manabe, S.: The influence of continental ice, atmospheric CO2, and land
1494 albedo on the climate of the last glacial maximum, Clim. Dyn., 1(2), 87–99,
1495 doi:10.1007/BF01054478, 1987.
1496 Bush, A. B. G., George, S. and Philander, H.: The late Cretaceous ’ Simulation with a coupled
1497 atmosphere-ocean general circulation model, , 12(3), 495–516, 1997.
1498 Charney, J., Arakawa, A., Baker, D. ., Bolin, B., Dickinson, R. E., Goody, R. ., Leith, C. .,
1499 Stommel, H. . and Wunsch, C. .: Carbon Dioxide and Climate, National Academies Press,
1500 Washington, D.C., 1979.
1501 Contoux, C., Jost, A., Ramstein, G., Sepulchre, P., Krinner, G. and Schuster, M.: Megalake
1502 chad impact on climate and vegetation during the late Pliocene and the mid-Holocene, Clim.
1503 Past, 9(4), 1417–1430, doi:10.5194/cp-9-1417-2013, 2013.
1504 Contoux, C., Dumas, C., Ramstein, G., Jost, A. and Dolan, A. M.: Modelling Greenland ice
1505 sheet inception and sustainability during the Late Pliocene, Earth Planet. Sci. Lett., 424, 295–

305, doi:10.1016/j.epsl.2015.05.018, 2015.
Crowley, T. J. and Berner, R. A.: CO2 and climate change, Science (80-. )., 292(5518), 870–872, doi:10.1126/science.1061664, 2001.
Crowley, T. J. and Zachos, J. C.: Comparison of zonal temperature profiles for past warm time periods, in Warm Climates in Earth History, edited by B. T. Huber, K. G. Macleod, and S. L. Wing, pp. 50–76, Cambridge University Press, Cambridge., 1999.
Crowley, T. J., Short, D. A., Mengel, J. G. and North, G. R.: Role of seasonality in the evolution of climate during the last 100 million years, Science (80-. )., 231(4738), 579–584, doi:10.1126/science.231.4738.579, 1986.
Damsté, J. S. S., Kuypers, M. M. M., Pancost, R. D. and Schouten, S.: The carbon isotopic response of algae, (cyano)bacteria, archaea and higher plants to the late Cenomanian perturbation of the global carbon cycle: Insights from biomarkers in black shales from the Cape Verde Basin (DSDP Site 367), Org. Geochem., 39(12), 1703–1718, doi:10.1016/j.orggeochem.2008.01.012, 2008.
Deconto, R. M., Brady, E. C., Bergengren, J. and Hay, W. W.: Late Cretaceous climate, vegetation, and ocean interactions, Warm Clim. Earth Hist., 275–296, doi:10.1017/cbo9780511564512.010, 2000.
Von Deimling, T. S., Ganopolski, A., Held, H. and Rahmstorf, S.: How cold was the last Glacial maximum?, Geophys. Res. Lett., 33(14), 1–5, doi:10.1029/2006GL026484, 2006.
Donnadieu, Y., Pierrehumbert, R., Jacob, R. and Fluteau, F.: Modelling the primary control of paleogeography on Cretaceous climate, Earth Planet. Sci. Lett., 248(1–2), 411–422, doi:10.1016/j.epsl.2006.06.007, 2006.
Dufresne, J. L., Foujols, M. A., Denvil, S., Caubel, A., Marti, O., Aumont, O., Balkanski, Y., Bekki, S., Bellenger, H., Benshila, R., Bony, S., Bopp, L., Braconnot, P., Brockmann, P., Cadule, P., Cheruy, F., Codron, F., Cozic, A., Cugnet, D., de Noblet, N., Duvel, J. P., Ethé, C., Fairhead, L., Fichefet, T., Flavoni, S., Friedlingstein, P., Grandpeix, J. Y., Guez, L., Guilyardi, E., Hauglustaine, D., Hourdin, F., Idelkadi, A., Ghattas, J., Joussaume, S., Kageyama, M., Krinner, G., Labetoulle, S., Lahellec, A., Lefebvre, M. P., Lefevre, F., Levy, C., Li, Z. X., Lloyd, J., Lott, F., Madec, G., Mancip, M., Marchand, M., Masson, S., Meurdesoif, Y., Mignot, J., Musat, I., Parouty, S., Polcher, J., Rio, C., Schulz, M., Swingedouw, D., Szopa, S., Talandier, C., Terray, P., Viovy, N. and Vuichard, N.: Climate change projections using the IPSL-CM5 Earth System Model: From CMIP3 to CMIP5., 2013.
Egbert, G. D., Ray, R. D. and Bills, B. G.: Numerical modeling of the global semidiurnal tide in the present day and in the last glacial maximum, J. Geophys. Res. C Ocean., 109(3), 1–15,

doi:10.1029/2003jc001973, 2004.
Enderton, D. and Marshall, J.: Explorations of Atmosphere–Ocean–Ice Climates on an Aquaplanet and Their Meridional Energy Transports, J. Atmos. Sci., 66(6), 1593–1611, doi:10.1175/2008jas2680.1, 2008.
Fichefet, T. and Maqueda, M. A. M.: Sensitivity of a global sea ice model to the treatment of ice thermodynamics and dynamics, J. Geophys. Res. Ocean., 102(C6), 12609–12646, doi:10.1029/97JC00480, 1997.
Fletcher, B. J., Brentnall, S. J., Quick, W. P. and Beerling, D. J.: BRYOCARB: A process-based model of thallose liverwort carbon isotope fractionation in response to CO2, O2, light and temperature, Geochim. Cosmochim. Acta, 70(23 SPEC. ISS.), 5676–5691, doi:10.1016/j.gca.2006.01.031, 2006.
Fluteau, F., Ramstein, G., Besse, J., Guiraud, R. and Masse, J. P.: Impacts of palaeogeography and sea level changes on Mid-Cretaceous climate, Palaeogeogr. Palaeoclimatol. Palaeoecol., 247(3–4), 357–381, doi:10.1016/j.palaeo.2006.11.016, 2007.
Foster, G. L., Royer, D. L. and Lunt, D. J.: Future climate forcing potentially without precedent in the last 420 million years, Nat. Commun., 8, 1–8, doi:10.1038/ncomms14845, 2017.
Friedrich, O., Norris, R. D. and Erbacher, J.: Evolution of middle to late Cretaceous oceans-A 55 m.y. Record of Earth's temperature and carbon cycle, Geology, 40(2), 107–110, doi:10.1130/G32701.1, 2012.
Gastineau, G., D'Andrea, F. and Frankignoul, C.: Atmospheric response to the North Atlantic Ocean variability on seasonal to decadal time scales, Clim. Dyn., 40(9–10), 2311–2330, doi:10.1007/s00382-012-1333-0, 2013.
Gates, W. L., Boyle, J. S., Covey, C., Dease, C. G., Doutriaux, C. M., Drach, R. S., Fiorino, M., Gleckler, P. J., Hnilo, J. J., Marlais, S. M., Phillips, T. J., Potter, G. L., Santer, B. D., Sperber, K. R., Taylor, K. E. and Williams, D. N.: An Overview of the Results of the Atmospheric Model Intercomparison Project (AMIP I), Bull. Am. Meteorol. Soc., 80(1), 29–55 [online] Available from: http://www.jstor.org/stable/26214897, 1999.
Goddéris, Y., Donnadieu, Y., Le Hir, G., Lefebvre, V. and Nardin, E.: The role of palaeogeography in the Phanerozoic history of atmospheric CO2and climate, Earth-Science Rev., 128, 122–138, doi:10.1016/j.earscirev.2013.11.004, 2014.
Golaz, J., Caldwell, P. M., Van Roekel, L. P., Petersen, M. R., Tang, Q., Wolfe, J. D., Abeshu, G., Anantharaj, V., Asay-Davis, X. S., Bader, D. C., Baldwin, S. A., Bisht, G., Bogenschutz, P. A., Branstetter, M., Brunke, M. A., Brus, S. R., Burrows, S. M., Cameron-

Smith, P. J., Donahue, A. S., Deakin, M., Easter, R. C., Evans, K. J., Feng, Y., Flanner, M., Foucar, J. G., Fyke, J. G., Griffin, B. M., Hannay, C., Harrop, B. E., Hunke, E. C., Jacob, R. L., Jacobsen, D. W., Jeffery, N., Jones, P. W., Keen, N. D., Klein, S. A., Larson, V. E., Leung, L. R., Li, H., Lin, W., Lipscomb, W. H., Ma, P., Mahajan, S., Maltrud, M. E., Mametjanov, A., McClean, J. L., McCoy, R. B., Neale, R. B., Price, S. F., Qian, Y., Rasch, P. J., Reeves Eyre, J. E. J., Riley, W. J., Ringler, T. D., Roberts, A. F., Roesler, E. L., Salinger, A. G., Shaheen, Z., Shi, X., Singh, B., Tang, J., Taylor, M. A., Thornton, P. E., Turner, A. K., Veneziani, M., Wan, H., Wang, H., Wang, S., Williams, D. N., Wolfram, P. J., Worley, P. H., Xie, S., Yang, Y., Yoon, J., Zelinka, M. D., Zender, C. S., Zeng, X., Zhang, C., Zhang, K., Zhang, Y., Zheng, X., Zhou, T. and Zhu, Q.: The DOE E3SM coupled model version 1: Overview and evaluation at standard resolution, J. Adv. Model. Earth Syst., 1–82, doi:10.1029/2018ms001603, 2019.

Goldner, A., Herold, N. and Huber, M.: Antarctic glaciation caused ocean circulation changes at the Eocene-Oligocene transition, Nature, 511(7511), 574–577, doi:10.1038/nature13597, 2014.

Gough: Solar interior structure variations*, Sol. Phys., 74(September 1980), 21–34, 1981.

Green, J. A. M. and Huber, M.: Tidal dissipation in the early Eocene and implications for ocean mixing, Geophys. Res. Lett., 40(11), 2707–2713, doi:10.1002/grl.50510, 2013.

Gyllenhaal, E. D., Engberts, C. J., Markwick, P. J., Smith, L. H. and Patzkowsky, M. E.: The Fujita-Ziegler model: a new semi-quantitative technique for estimating paleoclimate from paleogeographic maps, Palaeogeogr. Palaeoclimatol. Palaeoecol., 86(1–2), 41–66, doi:10.1016/0031-0182(91)90005-C, 1991.

Hay, W. W., DeConto, R. M., de Boer, P., Flögel, S., Song, Y. and Stepashko, A.: Possible solutions to several enigmas of Cretaceous climate, Springer Berlin Heidelberg., 2019.

Heinemann, M., Jungclaus, J. H. and Marotzke, J.: Warm Paleocene/Eocene climate as simulated in ECHAM5/MPI-OM, Clim. Past, 5(4), 785–802, doi:10.5194/cp-5-785-2009, 2009.

Herman, A. B. and Spicer, R. A.: Palaeobotanical evidence for a warm Cretaceous Arctic Ocean, Nature, 380(6572), 330–333, doi:10.1038/380330a0, 1996.

Herman, A. B. and Spicer, R. A.: Mid-Cretaceous floras and climate of the Russian high Arctic (Novosibirsk Islands, Northern Yakutiya), Palaeogeogr. Palaeoclimatol. Palaeoecol., 295(3–4), 409–422, doi:10.1016/j.palaeo.2010.02.034, 2010.

Herweijer, C., Seager, R., Winton, M. and Clement, A.: Why ocean heat transport warms the global mean climate, Tellus, Ser. A Dyn. Meteorol. Oceanogr., 57(4), 662–675,

1608 doi:10.1111/j.1600-0870.2005.00121.x, 2005.
1609 Hollis, C. J., Taylor, K. W. R., Handley, L., Pancost, R. D., Huber, M., Creech, J. B., Hines,
1610 B. R., Crouch, E. M., Morgans, H. E. G., Crampton, J. S., Gibbs, S., Pearson, P. N. and
1611 Zachos, J. C.: Early Paleogene temperature history of the Southwest Pacific Ocean :
1612 Reconciling proxies and models, Earth Planet. Sci. Lett., 349–350, 53–66,
1613 doi:10.1016/j.epsl.2012.06.024, 2012.
1614 Hong, S. K. and Lee, Y. Il: Evaluation of atmospheric carbon dioxide concentrations during
1615 the Cretaceous, Earth Planet. Sci. Lett., 327–328, 23–28, doi:10.1016/j.epsl.2012.01.014,
1616 2012.
1617 Hotinski, R. M. and Toggweiler, J. R.: Impact of a Tethyan circumglobal passage on ocean
1618 heat transport and "equable" climates, Paleoceanography, 18(1), n/a-n/a,
1619 doi:10.1029/2001PA000730, 2003.
1620 Hourdin, F., Foujols, M. A., Codron, F., Guemas, V., Dufresne, J. L., Bony, S., Denvil, S.,
1621 Guez, L., Lott, F., Ghattas, J., Braconnot, P., Marti, O., Meurdesoif, Y. and Bopp, L.: Impact
1622 of the LMDZ atmospheric grid configuration on the climate and sensitivity of the IPSL-
1623 CM5A coupled model, Clim. Dyn., 40(9–10), 2167–2192, doi:10.1007/s00382-012-1411-3,
1624 2013.
1625 Huber, B. T., Hodell, D. A. and Hamilton, C. P.: … Late Cretaceous climate of the southern
1626 high latitudes: Stable isotopic evidence for minimal …, Geol. Soc. Am. Bull., (10), 1164–
1627 1191, doi:10.1130/0016-7606(1995)107<1164, 1995.
1628 Huber, B. T., Leckie, R. M., Norris, R. D., Bralower, T. J. and CoBabe, E.: Foraminiferal
1629 assemblage and stable isotopic change across the Cenomanian-Turonian boundary in the
1630 Subtropical North Atlantic, J. Foraminifer. Res., 29(4), 392–417, 1999.
1631 Huber, B. T., Norris, R. D. and MacLeod, K. G.: Deep-sea paleotemperature record of
1632 extreme warmth during the Cretaceous, Geology, 30(2), 123–126, doi:10.1130/0091-
1633 7613(2002)030<0123:DSPROE>2.0.CO;2, 2002.
1634 Huber, B. T., MacLeod, K. G., Watkins, D. K. and Coffin, M. F.: The rise and fall of the
1635 Cretaceous Hot Greenhouse climate, Glob. Planet. Change, 167(April), 1–23,
1636 doi:10.1016/j.gloplacha.2018.04.004, 2018.
1637 Huber, M.: Progress in Greenhouse Climate Modeling, Paleontol. Soc. Pap., 18, 213–262,
1638 doi:10.1017/s108933260000262x, 2012.
1639 Huber, M. and Caballero, R.: The early Eocene equable climate problem revisited, Clim. Past,
1640 7(2), 603–633, doi:10.5194/cp-7-603-2011, 2011.
1641 Hunter, S. J., Haywood, A. M., Valdes, P. J., Francis, J. E. and Pound, M. J.: Modelling

equable climates of the Late Cretaceous: Can new boundary conditions resolve data-model discrepancies?, Palaeogeogr. Palaeoclimatol. Palaeoecol., 392, 41–51, doi:10.1016/j.palaeo.2013.08.009, 2013.
Hutchinson, D. K., De Boer, A. M., Coxall, H. K., Caballero, R., Nilsson, J. and Baatsen, M.: Climate sensitivity and meridional overturning circulation in the late Eocene using GFDL CM2.1, Clim. Past, 14(6), 789–810, doi:10.5194/cp-14-789-2018, 2018.
IPCC: Climate Change 2014: Synthesis Report. Contribution of Working Groups I, II and III to the Fifth Assessment Report of the Intergovernmental Panel on Climate Change., 2014.
Jenkyns, H. C.: Geochemistry of oceanic anoxic events, Geochemistry, Geophys. Geosystems, 11(3), 1–30, doi:10.1029/2009GC002788, 2010.
Jenkyns, H. C., Forster, A., Schouten, S. and Sinninghe Damsté, J. S.: High temperatures in the Late Cretaceous Arctic Ocean, Nature, 432(7019), 888–892, doi:10.1038/nature03143, 2004.
Kageyama, M., Braconnot, P., Bopp, L., Caubel, A., Foujols, M. A., Guilyardi, E., Khodri, M., Lloyd, J., Lombard, F., Mariotti, V., Marti, O., Roy, T. and Woillez, M. N.: Mid-Holocene and Last Glacial Maximum climate simulations with the IPSL model-part I: Comparing IPSL_CM5A to IPSL_CM4, Clim. Dyn., 40(9–10), 2447–2468, doi:10.1007/s00382-012-1488-8, 2013.
Kennedy, A. T., Farnsworth, A., Lunt, D. J., Lear, C. H. and Markwick, P. J.: Atmospheric and oceanic impacts of Antarctic glaciation across the Eocene-Oligocene transition, Philos. Trans. R. Soc. A Math. Phys. Eng. Sci., 373(2054), doi:10.1098/rsta.2014.0419, 2015.
Kerr, A. C. and Kerr, A. C.: Oceanic plateau formation : A cause of mass extinction and black shale deposition around the Cenomanian-Turonian boundary ? Oceanic plateau formation : a cause of mass extinction and black shale deposition around the Cenomanian – Turonian boundary ?, , (May), doi:10.1144/gsjgs.155.4.0619, 1998.
Knorr, G. and Lohmann, G.: Climate warming during antarctic ice sheet expansion at the middle miocene transition, Nat. Geosci., 7(5), 376–381, doi:10.1038/ngeo2119, 2014.
Koch-Larrouy, A., Madec, G., Bouruet-Aubertot, P., Gerkema, T., Bessières, L. and Molcard, R.: On the transformation of Pacific Water into Indonesian Throughflow Water by internal tidal mixing, Geophys. Res. Lett., 34(4), 1–6, doi:10.1029/2006GL028405, 2007.
Krinner, G., Viovy, N., de Noblet-Ducoudré, N., Ogée, J., Polcher, J., Friedlingstein, P., Ciais, P., Sitch, S. and Prentice, I. C.: A dynamic global vegetation model for studies of the coupled atmosphere-biosphere system, Global Biogeochem. Cycles, 19(1), 1–33, doi:10.1029/2003GB002199, 2005.

1676 Ladant, J. B. and Donnadieu, Y.: Palaeogeographic regulation of glacial events during the
1677 Cretaceous supergreenhouse, Nat. Commun., 7(April 2017), 1–9, doi:10.1038/ncomms12771,
1678 2016.
1679 Ladant, J. B., Donnadieu, Y., Bopp, L., Lear, C. H. and Wilson, P. A.: Meridional Contrasts
1680 in Productivity Changes Driven by the Opening of Drake Passage, Paleoceanogr.
1681 Paleoclimatology, 302–317, doi:10.1002/2017PA003211, 2018.
1682 de Lavergne, C., Falahat, S., Madec, G., Roquet, F., Nycander, J. and Vic, C.: Toward global
1683 maps of internal tide energy sinks, Ocean Model., 137(April), 52–75,
1684 doi:10.1016/j.ocemod.2019.03.010, 2019.
1685 Leier, A., Quade, J., DeCelles, P. and Kapp, P.: Stable isotopic results from paleosol
1686 carbonate in South Asia: Paleoenvironmental reconstructions and selective alteration, Earth
1687 Planet. Sci. Lett., 279(3–4), 242–254, doi:10.1016/j.epsl.2008.12.044, 2009.
1688 Levine, X. J. and Schneider, T.: Response of the Hadley Circulation to Climate Change in an
1689 Aquaplanet GCM Coupled to a Simple Representation of Ocean Heat Transport, J. Atmos.
1690 Sci., 68(4), 769–783, doi:10.1175/2010jas3553.1, 2010.
1691 Littler, K., Robinson, S. A., Bown, P. R., Nederbragt, A. J. and Pancost, R. D.: High sea-
1692 surface temperatures during the Early Cretaceous Epoch, Nat. Geosci., 4(3), 169–172,
1693 doi:10.1038/ngeo1081, 2011.
1694 Lunt, D. J., Jones, T. D., Heinemann, M., Huber, M., LeGrande, A., Winguth, A., Loptson,
1695 C., Marotzke, J., Roberts, C. D., Tindall, J., Valdes, P. and Winguth, C.: A model-data
1696 comparison for a multi-model ensemble of early Eocene atmosphere-ocean simulations:
1697 EoMIP, Clim. Past, 8(5), 1717–1736, doi:10.5194/cp-8-1717-2012, 2012a.
1698 Lunt, D. J., Haywood, A. M., Schmidt, G. A., Salzmann, U., Valdes, P. J., Dowsett, H. J. and
1699 Loptson, C. A.: On the causes of mid-Pliocene warmth and polar amplification, Earth Planet.
1700 Sci. Lett., 321–322, 128–138, doi:10.1016/j.epsl.2011.12.042, 2012b.
1701 Lunt, D. J., Farnsworth, A., Loptson, C., L Foster, G., Markwick, P., O'Brien, C. L., Pancost,
1702 R. D., Robinson, S. A. and Wrobel, N.: Palaeogeographic controls on climate and proxy
1703 interpretation, Clim. Past, 12(5), 1181–1198, doi:10.5194/cp-12-1181-2016, 2016.
1704 Lunt, D. J., Huber, M., Anagnostou, E., Baatsen, M. L. J., Caballero, R., DeConto, R.,
1705 Dijkstra, H. A., Donnadieu, Y., Evans, D., Feng, R., Foster, G. L., Gasson, E., Von Der
1706 Heydt, A. S., Hollis, C. J., Inglis, G. N., Jones, S. M., Kiehl, J., Turner, S. K., Korty, R. L.,
1707 Kozdon, R., Krishnan, S., Ladant, J. B., Langebroek, P., Lear, C. H., LeGrande, A. N., Littler,
1708 K., Markwick, P., Otto-Bliesner, B., Pearson, P., Poulsen, C. J., Salzmann, U., Shields, C.,
1709 Snell, K., Stärz, M., Super, J., Tabor, C., Tierney, J. E., Tourte, G. J. L., Tripati, A.,

1710 Upchurch, G. R., Wade, B. S., Wing, S. L., Winguth, A. M. E., Wright, N. M., Zachos, J. C.
1711 and Zeebe, R. E.: The DeepMIP contribution to PMIP4: Experimental design for model
1712 simulations of the EECO, PETM, and pre-PETM (version 1.0), Geosci. Model Dev., 10(2),
1713 889–901, doi:10.5194/gmd-10-889-2017, 2017.
1714 MacLeod, K. G., Huber, B. T., Berrocoso, Á. J. and Wendler, I.: A stable and hot Turonian
1715 without glacial δ18O excursions is indicated by exquisitely preserved Tanzanian foraminifera,
1716 Geology, 41(10), 1083–1086, doi:10.1130/G34510.1, 2013.
1717 Madec, G.: NEMO ocean engine (2012), , (27), 2012.
1718 Madec, G. and Imbard, M.: A global ocean mesh to overcome the North Pole singularity,
1719 Clim. Dyn., 12(6), 381–388, doi:10.1007/BF00211684, 1996.
1720 Maffre, P., Ladant, J. B., Donnadieu, Y., Sepulchre, P. and Goddéris, Y.: The influence of
1721 orography on modern ocean circulation, Clim. Dyn., 50(3–4), 1277–1289,
1722 doi:10.1007/s00382-017-3683-0, 2018.
1723 Mays, C., Steinthorsdottir, M. and Stilwell, J. D.: Climatic implications of Ginkgoites
1724 waarrensis Douglas emend. from the south polar Tupuangi flora, Late Cretaceous
1725 (Cenomanian), Chatham Islands, Palaeogeogr. Palaeoclimatol. Palaeoecol., 438, 308–326,
1726 doi:10.1016/j.palaeo.2015.08.011, 2015.
1727 Le Mézo, P., Beaufort, L., Bopp, L., Braconnot, P. and Kageyama, M.: From monsoon to
1728 marine productivity in the Arabian Sea: Insights from glacial and interglacial climates, Clim.
1729 Past, 13(7), 759–778, doi:10.5194/cp-13-759-2017, 2017.
1730 Monteiro, F. M., Pancost, R. D., Ridgwell, A. and Donnadieu, Y.: Nutrients as the dominant
1731 control on the spread of anoxia and euxinia across the Cenomanian-Turonian oceanic anoxic
1732 event (OAE2): Model-data comparison, Paleoceanography, 27(4), 1–17,
1733 doi:10.1029/2012PA002351, 2012.
1734 Müller, R. D., Sdrolias, M., Gaina, C. and Roest, W. R.: Age, spreading rates, and spreading
1735 asymmetry of the world's ocean crust, Geochemistry, Geophys. Geosystems, 9(4), 1–19,
1736 doi:10.1029/2007GC001743, 2008.
1737 Niezgodzki, I., Knorr, G., Lohmann, G., Tyszka, J. and Markwick, P. J.: Late Cretaceous
1738 climate simulations with different CO2 levels and subarctic gateway configurations: A model-
1739 data comparison, Paleoceanography, 32(9), 980–998, doi:10.1002/2016PA003055, 2017.
1740 Norris, R. D., Bice, K. L., Magno, E. A. and Wilson, P. A.: Jiggling the tropical thermostat in
1741 the Cretaceous hothouse, Geology, 30(4), 299–302, doi:10.1130/0091-
1742 7613(2002)030<0299:JTTTIT>2.0.CO;2, 2002.
1743 O'Brien, C. L., Robinson, S. A., Pancost, R. D., Sinninghe Damsté, J. S., Schouten, S., Lunt,

D. J., Alsenz, H., Bornemann, A., Bottini, C., Brassell, S. C., Farnsworth, A., Forster, A., Huber, B. T., Inglis, G. N., Jenkyns, H. C., Linnert, C., Littler, K., Markwick, P., McAnena, A., Mutterlose, J., Naafs, B. D. A., Püttmann, W., Sluijs, A., van Helmond, N. A. G. M., Vellekoop, J., Wagner, T. and Wrobel, N. E.: Cretaceous sea-surface temperature evolution: Constraints from TEX 86 and planktonic foraminiferal oxygen isotopes, Earth-Science Rev., 172(March 2016), 224–247, doi:10.1016/j.earscirev.2017.07.012, 2017.

Ohba, M. and Ueda, H.: A GCM Study on Effects of Continental Drift on Tropical Climate at the Early and Late Cretaceous, J. Meteorol. Soc. Japan, 88(6), 869–881, doi:10.2151/jmsj.2010-601, 2011.

Ortega, P., Mignot, J., Swingedouw, D., Sévellec, F. and Guilyardi, E.: Reconciling two alternative mechanisms behind bi-decadal variability in the North Atlantic, Prog. Oceanogr., 137, 237–249, doi:10.1016/j.pocean.2015.06.009, 2015.

Otto-bliesner, B. L. and Upchurch, G. R.: the Late Cretaceous period, , 385127(February), 18–21, 1997.

Pearson, P. N., DitchfieldPeter, W., SinganoJoyce, Harcourt-BrownKatherine, G., NicholasChristopher, J., OlssonRichard, K., ShackletonNicholas, J. and HallMike, A.: erratum: Warm tropical sea surface temperatures in the Late Cretaceous and Eocene epochs, Nature, 414(6862), 470 [online] Available from: http://dx.doi.org/10.1038/35106617, 2001.

Poulsen, C. J., Seidov, D., Barron, E. J. and Peterson, W. H.: The impact of paleogeographic evolution on the surface oceanic circulation and the marine environment within the Mid-Cretaceous tethys, , 13(5), 546–559, 1998.

Poulsen, C. J., Barron, E. J., Arthur, M. A. and Peterson, W. H.: Response of the mid-Cretaceous global oceanic circulation to tectonic and CO<inf>2</inf> forcings, Paleoceanography, 16(6), 576–592, doi:10.1029/2000PA000579, 2001.

Poulsen, C. J., Gendaszek, A. S. and Jacob, R. L.: Did the rifting of the Atlantic Ocean cause the Cretaceous thermal maximum?, Geology, 31(2), 115–118, doi:10.1130/0091-7613(2003)031<0115:DTROTA>2.0.CO;2, 2003.

Poulsen, C. J., Pollard, D. and White, T. S.: General circulation model simulation of the δ18O content of continental precipitation in the middle Cretaceous: A model-proxy comparison, Geology, 35(3), 199–202, doi:10.1130/G23343A.1, 2007.

Pucéat, E., Lécuyer, C., Donnadieu, Y., Naveau, P., Cappetta, H., Ramstein, G., Huber, B. T. and Kriwet, J.: Fish tooth δ18O revising Late Cretaceous meridional upper ocean water temperature gradients, Geology, 35(2), 107–110, doi:10.1130/G23103A.1, 2007.

Retallack, G. J. and Conde, G. D.: Deep time perspective on rising atmospheric CO2, Glob.

Planet. Change, 189(March), 103177, doi:10.1016/j.gloplacha.2020.103177, 2020.
Robinson, S. A., Dickson, A. J., Pain, A., Jenkyns, H. C., O'Brien, C. L., Farnsworth, A. and Lunt, D. J.: Southern Hemisphere sea-surface temperatures during the Cenomanian-Turonian: Implications for the termination of Oceanic Anoxic Event 2, Geology, 47(2), 131–134, doi:10.1130/G45842.1, 2019.
Rose, B. E. J. and Ferreira, D.: Ocean heat transport and water vapor greenhouse in a warm equable climate: A new look at the low gradient paradox, J. Clim., 26(6), 2117–2136, doi:10.1175/JCLI-D-11-00547.1, 2013.
Royer, D. L.: Atmospheric CO2 and O2 During the Phanerozoic: Tools, Patterns, and Impacts, 2nd ed., Elsevier Ltd., 2013.
Royer, D. L., Berner, R. A. and Park, J.: Climate sensitivity constrained by CO2 concentrations over the past 420 million years, Nature, 446(7135), 530–532, doi:10.1038/nature05699, 2007.
Sandler, A. and Harlavan, Y.: Early diagenetic illitization of illite-smectite in Cretaceous sediments (Israel): evidence from K-Ar dating, Clay Miner., 41(2), 637–658, doi:10.1180/0009855064120210, 2006.
Sarr, A. C., Sepulchre, P. and Husson, L.: Impact of the Sunda Shelf on the Climate of the Maritime Continent, J. Geophys. Res. Atmos., doi:10.1029/2018JD029971, 2019.
Schmidt, G. A. and Mysak, L. A.: Can increased poleward oceanic heat flux explain the warm Cretaceous climate?, Paleoceanography, 11(5), 579–593, doi:10.1029/96PA01851, 1996.
Sellers, P. ., Bounoua, L., Collatz, G. J., Randall, D. A., Dazlich, D. A., Los, S. O., Berry, J. A., Fung, I., Tucker, C. J., Field, C. B. and Jensen, T. G.: Comparison of Radiative and Physiological Effects of Doubled Atmospheric CO2 on Climate, , 1402–1406, 1996.
Sellwood, B. W., Price, G. D. and Valdest, P. J.: Cretaceous temperatures, , 370(August), 453–455, 1994.
Sepulchre, P., Caubel, A., Ladant, J., Bopp, L., Boucher, O., Braconnot, P., Brockmann, P., Cozic, A., Donnadieu, Y., Estella-perez, V., Ethé, C., Fluteau, F., Foujols, M., Gastineau, G., Ghattas, J., Hauglustaine, D., Hourdin, F., Kageyama, M., Khodri, M., Marti, O., Meurdesoif, Y., Mignot, J., Sarr, A., Servonnat, J., Swingedouw, D., Szopa, S. and Tardif, D.: IPSL-CM5A2 . An Earth System Model designed for multi-millennial climate simulations, , (December), 2019.
Sewall, J. O., Van De Wal, R. S. W., Van Der Zwan, K., Van Oosterhout, C., Dijkstra, H. A. and Scotese, C. R.: Climate model boundary conditions for four Cretaceous time slices, Clim. Past, 3(4), 647–657, doi:10.5194/cp-3-647-2007, 2007.

1812 Simmons, H. L., Jayne, S. R., St. Laurent, L. C. and Weaver, A. J.: Tidally driven mixing in a
1813 numerical model of the ocean general circulation, Ocean Model., 6(3–4), 245–263,
1814 doi:10.1016/S1463-5003(03)00011-8, 2004.
1815 Sluijs, A., Schouten, S., Pagani, M., Woltering, M. and Brinkhuis, H.: Subtropical Arctic
1816 Ocean temperatures during the Palaeocene / Eocene thermal maximum, , (May 2014),
1817 doi:10.1038/nature04668, 2006.
1818 Spicer, R. A. and Herman, A. B.: The Late Cretaceous environment of the Arctic: A
1819 quantitative reassessment based on plant fossils, Palaeogeogr. Palaeoclimatol. Palaeoecol.,
1820 295(3–4), 423–442, doi:10.1016/j.palaeo.2010.02.025, 2010.
1821 Steinig, S., Dummann, W., Park, W., Latif, M., Kusch, S., Hofmann, P. and Flögel, S.:
1822 Evidence for a regional warm bias in the Early Cretaceous TEX86 record, Earth Planet. Sci.
1823 Lett., 539, 116184, doi:10.1016/j.epsl.2020.116184, 2020.
1824 Swingedouw, D., Rodehacke, C. B., Olsen, S. M., Menary, M., Gao, Y., Mikolajewicz, U.
1825 and Mignot, J.: On the reduced sensitivity of the Atlantic overturning to Greenland ice sheet
1826 melting in projections: a multi-model assessment, Clim. Dyn., 44(11–12), 3261–3279,
1827 doi:10.1007/s00382-014-2270-x, 2015.
1828 Swingedouw, D., Mignot, J., Guilyardi, E., Nguyen, S. and Ormières, L.: Tentative
1829 reconstruction of the 1998–2012 hiatus in global temperature warming using the IPSL–
1830 CM5A–LR climate model, Comptes Rendus - Geosci., 349(8), 369–379,
1831 doi:10.1016/j.crte.2017.09.014, 2017.
1832 Tabor, C. R., Poulsen, C. J., Lunt, D. J., Rosenbloom, N. A., Otto-Bliesner, B. L., Markwick,
1833 P. J., Brady, E. C., Farnsworth, A. and Feng, R.: The cause of Late Cretaceous cooling: A
1834 multimodel-proxy comparison, Geology, 44(11), 963–966, doi:10.1130/G38363.1, 2016.
1835 Tagliabue, A., Bopp, L., Dutay, J. C., Bowie, A. R., Chever, F., Jean-Baptiste, P., Bucciarelli,
1836 E., Lannuzel, D., Remenyi, T., Sarthou, G., Aumont, O., Gehlen, M. and Jeandel, C.:
1837 Hydrothermal contribution to the oceanic dissolved iron inventory, Nat. Geosci., 3(4), 252–
1838 256, doi:10.1038/ngeo818, 2010.
1839 Tan, N., Ramstein, G., Dumas, C., Contoux, C., Ladant, J. B., Sepulchre, P., Zhang, Z. and
1840 De Schepper, S.: Exploring the MIS M2 glaciation occurring during a warm and high
1841 atmospheric CO2Pliocene background climate, Earth Planet. Sci. Lett., 472, 266–276,
1842 doi:10.1016/j.epsl.2017.04.050, 2017.
1843 Tierney, J. E.: GDGT Thermometry: Lipid Tools for Reconstructing Paleotemperatures,
1844 Paleontol. Soc. Pap., 18, 115–132, doi:10.1017/s1089332600002588, 2012.
1845 Turgeon, S. C. and Creaser, R. A.: Cretaceous oceanic anoxic event 2 triggered by a massive

magmatic episode, , 454(July), doi:10.1038/nature07076, 2008.
Upchurch, G. R.: Vegetation-atmosphere interactions and their role in global warming during the latest Cretaceous, Philos. Trans. R. Soc. B Biol. Sci., 353(1365), 97–112, doi:10.1098/rstb.1998.0194, 1998.
Upchurch, G. R., Kiehl, J., Shields, C., Scherer, J. and Scotese, C.: Latitudinal temperature gradients and high-latitude temperatures during the latest Cretaceous: Congruence of geologic data and climate models, Geology, 43(8), 683–686, doi:10.1130/G36802.1, 2015.
Valcke, S., Budich, R., Carter, M., Guilyardi, E., Lautenschlager, M., Redler, R. and Steenman-clark, L.: The PRISM software framework and the OASIS coupler, , 5(September 2014), 2001–2004, 2006.
Vandermark, D., Tarduno, J. A. and Brinkman, D. B.: A fossil champsosaur population from the high Arctic: Implications for Late Cretaceous paleotemperatures, Palaeogeogr. Palaeoclimatol. Palaeoecol., 248(1–2), 49–59, doi:10.1016/j.palaeo.2006.11.008, 2007.
Veizer, J., Godderis, Y. and François, L. M.: Evidence for decoupling of atmospheric CO 2 and global climate during the Phanerozoic eon, Nature, 408(6813), 698–701, doi:10.1038/35047044, 2000.
Wang, Y., Huang, C., Sun, B., Quan, C., Wu, J. and Lin, Z.: Paleo-CO2 variation trends and the Cretaceous greenhouse climate, Earth-Science Rev., 129, 136–147, doi:10.1016/j.earscirev.2013.11.001, 2014.
Wilson, M. F. and Henderson-sellers, A.: LBA Regional Vegetation and Soils, 1-Degree (Wilson and Henderson-Sellers), , doi:10.3334/ORNLDAAC/687, 2003.
Woillez, M. N., Levavasseur, G., Daniau, A. L., Kageyama, M., Urrego, D. H., Sánchez-Goñi, M. F. and Hanquiez, V.: Impact of precession on the climate, vegetation and fire activity in southern Africa during MIS4, Clim. Past, 10(3), 1165–1182, doi:10.5194/cp-10-1165-2014, 2014.
Zhou, J., Poulsen, C. J., Pollard, D. and White, T. S.: Simulation of modern and middle Cretaceous marine δ18O with an ocean-atmosphere general circulation model, Paleoceanography, 23(3), 1–11, doi:10.1029/2008PA001596, 2008.
Zhou, J., Poulsen, C. J., Rosenbloom, N., Shields, C. and Briegleb, B.: Vegetation-climate interactions in the warm mid-Cretaceous, Clim. Past, 8(2), 565–576, doi:10.5194/cp-8-565-2012, 2012.
Zhu, J., Poulsen, C. J. and Tierney, J. E.: Simulation of Eocene extreme warmth and high climate sensitivity through cloud feedbacks, Sci. Adv., 5(9), eaax1874, doi:10.1126/sciadv.aax1874, 2019.

Zhu, J., Poulsen, C. J., Otto-Bliesner, B. L., Liu, Z., Brady, E. C. and Noone, D. C.: Simulation of early Eocene water isotopes using an Earth system model and its implication for past climate reconstruction, Earth Planet. Sci. Lett., 537, 116164, doi:10.1016/j.epsl.2020.116164, 2020.

Zobler, L.: Global Soil Types, 1-Degree Grid (Zobler), , doi:10.3334/ORNLDAAC/418, 1999.